

THE FLORIDA STATE UNIVERSITY
COLLEGE OF ARTS AND SCIENCES

A VARIATIONAL METHOD FOR
ASSIMILATION OF SCATTEROMETER
WINDS INTO SURFACE PRESSURE FIELDS

by

JACK HARLAN, JR.

A thesis submitted to the
Department of Oceanography
in partial fulfillment of the
requirements for the degree of
Master of Science



Approved:



Professor Directing Thesis





Chairman, Department of Oceanography

December, 1985

December, 1985

ABSTRACT

A variational formulation was used to assimilate conventional NMC sea level pressure fields and SEASAT-A scatterometer (SASS) surface wind measurements near and during the QE II storm. An estimate of the relative vorticity at every point on a grid was calculated using each of these two data sets. A solution to a modified geostrophic stream function is found subject to the constraints that 1) the relative vorticities calculated from the data agree as closely as possible with the relative vorticities from the variational solution; and 2) the average kinetic energy is a minimum. Results are obtained which support the idea that averaged satellite data can be treated as synoptic data. Direct substitution rather than a time-weighted insertion made from SASS winds generally resulted in more accurate pressure analyses. In addition, this relatively simple model provides surface pressure fields which agree extremely well with surface truth and the results of other investigators who required additional sources of input data into more complex models. It will be possible to obtain improved wind field maps from future scatterometer pressure fields in midlatitudes.

ACKNOWLEDGEMENTS

This work was supported by a NASA Traineeship Grant.

I wish to thank, first, Dr. James J. O'Brien for the opportunity to begin this work and his invaluable aid throughout its course. He also provided me with valuable summer experience at NCAR. There, Dr. William Large initiated this project. Many thanks to him for patient guidance and encouragement. Also, at NCAR, Wendell Nuss was extremely helpful and insightful. Special thanks also go to Dr. Benoit Cushman-Roisin and to Rick Chapman and Manual Lopez for their continued support and ideas. Finally, I wish to thank my family and my wife, Tracy; without whom this would not have been possible.

TABLE OF CONTENTS

	Page
ABSTRACT	ii
ACKNOWLEDGEMENTS	iii
TABLE OF CONTENTS	iv
LIST OF FIGURES	v
I. INTRODUCTION	1
II. DATA BASE AND DATA ANALYSIS TECHNIQUES	5
III. COMPARISON OF SEASAT WINDS AND GEOSTROPHIC WINDS	19
IV. ASSIMILATION TECHNIQUE BY A VARIATIONAL FORMULATION	28
V. RESULTS OF ASSIMILATION OF SEASAT WINDS	37
VI. SUMMARY AND CONCLUSIONS	57
REFERENCES	60

LIST OF FIGURES

		PAGE
Fig.1a	North Atlantic study region including SEASAT data points (dots) and NMC grid points (crosses). The square represents a typical area from which SASS vorticity estimate is obtained for the center grid point of the square. For September 9, 1978 1200 UT (OBS 7).	6
Fig.1b	Same as Fig. 1a but without square and for September 10, 1978 0000 UT (OBS 8).	7
Fig.1c	Same as Fig. 1a for September 10, 1978 1200 UT (OBS 9).	8
Fig.1d	Same as Fig. 1a for September 11, 1978 0000 UT (OBS 10).	9
Fig.1e	Same as Fig. 1a for September 11, 1978 1200 UT (OBS 11).	10
Fig.2a	NMC surface pressure analysis for September 9, 1978 1200 UT (OBS 7).	12
Fig.2b	NMC surface pressure analysis for September 10, 1978 0000 UT (OBS 8).	13
Fig.2b	NMC surface pressure analysis for September 10, 1978 0000 UT (OBS 8).	13

	PAGE
Fig.2c	NMC surface pressure analysis for September 10, 1978 1200 UT (OBS 9). 14
Fig.2d	NMC surface pressure analysis for September 11, 1978 0000 UT (OBS 10). 15
Fig.2e	NMC surface pressure analysis for September 11, 1978 1200 UT (OBS 11). 16
Fig.3a-b	SASS wind speed vs. reduced-rotated geostrophic winds for entire 6 hour time window and entire study area: (a) for OBS 7; $r^2 = 0.53$, (b) for OBS 8, $r^2 = 0.21$. 21
Fig.3c-d	SASS wind speed vs. reduced-rotated geostrophic winds for entire 6 hour time window and entire study area: (c) for OBS 9, $r^2 = 0.31$, (d) for OBS 10, $r^2 = 0.74$. Note different scale sizes. 22
Fig.3e	SASS wind speed vs. reduced-rotated geostrophic winds for entire 6 hour time window and entire study area: (e) for OBS 11, $r^2 = 0.67$. 23
Fig.4a-b	Same as Figs. 3 but for a subregion encompassing only the storm region: (a) for OBS 7, $r^2 = 0.04$, (b) for OBS 8, $r^2 = 0.01$. encompassing only the storm region: (a) for OBS 7, $r^2 = 0.04$, (b) for OBS 8, $r^2 = 0.01$. Note different scale sizes. 25

Fig.4c-d	Same as Figs. 3 but for a subregion encompassing only the storm region: (c) for OBS 9; $r^2 = 0.00$, (d) for OBS 10, $r^2 = 0.08$. Note different scale sizes.	26
Fig.4e	Same as Figs. 3 but for a subregion encompassing only the storm region: (e) for OBS 11, $r^2 = 0.42$.	27
Fig.5a	Adjusted surface pressure field after time-weighted insertion of SASS relative vorticities, OBS 7.	38
Fig.5b	Same as Fig. 5a but for OBS 8.	39
Fig.5c	Same as Fig. 5a but for OBS 9.	40
Fig.5d	Same as Fig. 5a but for OBS 10.	41
Fig.5e	Same as Fig. 5a but for OBS 11.	42
Fig.6a	Adjusted pressure field after substitution ($F_{ij} = 1.0$) of SASS relative vorticities.	44
Fig.6b	Same as Fig. 6a but for OBS 8.	45
Fig.6c Fig.6b	Same as Fig. 6a but for OBS 9.	46
Fig.6c	Same as Fig. 6a but for OBS 9.	46

		PAGE
Fig.6d	Same as Fig. 6a but for OBS 10.	47
Fig.6e	Same as fig. 6a but for OBS 11.	48
Fig.7	SASS wind vectors for OBS 10. Note that only every other vector has been plotted for clarity.	51
Fig.8	Same as Fig. 6a but for slightly larger size square.	54
Fig.9	Same as 6c but for slightly larger size square.	55

Introduction

Accurate weather forecasting over the ocean has long been hampered by the sparsity of observations made at sea. The inadequacy of the data, both in time and space, creates a handicap for numerical weather prediction models. Conventional data can now be supplemented with satellite data which are available at much higher spatial resolution although they are asynoptic.

The scatterometer radar on board the SEASAT satellite (SASS) provided wind vector data for approximately 100 days in 1978. These winds had a resolution of approximately 100km while meeting the pre-flight specifications of $\pm 2\text{ms}^{-1}$ or $\pm 10\%$ for wind speed and $\pm 20^\circ$ for wind direction (Lame and Born, 1982). Even though it has recently been shown (Woiceshyn et al., 1985) that the geophysical algorithms present in the wind retrieval system of SASS has some deficiencies for certain circumstances (e.g. low wind speeds over colder water), the SASS winds still remain as the most complete and accurate wind data set available for the time period during SEASAT's operation. Apart from errors in the geophysical algorithm, there is a directional ambiguity or "alias" present in the radar backscatter measurements. Four equivalent solutions for direction are typical. Numerous techniques have been used to de-alias these vectors.

Numerous techniques have been used to de-alias these vectors.

Hoffman (1982) used a variational method to objectively de-alias the SASS data. However, the method of Wurtele et al. (1982) provided the de-aliased wind vectors used in this study.

Yu and McPherson (1984) de-aliased the SASS winds in experiments which demonstrated a significant difference between forecasts made using SASS data and those made without are in the Southern Hemisphere where little conventional data are available. They were unable to conclude whether or not the difference was an improvement.

Because the problem of determining which surface pressure analysis is correct when using different sources of input data, i.e. with SASS data versus without SASS data, several studies have centered on the QE II storm which occurred on September 10, 1978 to September 11, 1978 in the North Atlantic causing extensive damage to the Queen Elizabeth II ocean liner. This storm is referred to as a "bomb" by Sanders and Gyakum (1980) due to the incredible rate at which its low pressure centered deepened. It changed approximately 60mb to a minimum pressure of around 945mb in 24 hours. Because the National Meteorological Center failed to provide an accurate prediction of the location or intensity of this storm and, since Seasat flew directly over the storm, this rather strong storm provides an opportunity to ascertain the effect of satellite scatterometer-derived winds on the surface pressure analysis. Fortunately, the surface truth for the storm is provided by the scatterometer-derived winds on the surface pressure analysis. Fortunately, the surface truth for the storm is provided by the

barograph tracing of the freighter Euroliner, which is believed to have passed through the center of the fully developed storm on September 10, 1978 1200 UT (Gyakum, 1983; see his Fig. 1).

The potential impact of SASS winds on the prediction of the QE II storm is pointed out by Cane and Cardone (1982). They illustrate the correct location and intensity of the storm superimposed by a satellite swath which occurs at very nearly the same time as the analysis of September 10, 1978 1200 UT. Duffy and Atlas (1985) were the first to assimilate the scatterometer data with a numerical weather prediction model to obtain an improved surface pressure field. Anthes et al. (1983) made use of SASS data in an extensive set of model simulations attempting to predict the QE II storm. However, since there are numerous input parameters and sources for data to these experiments, no clear assessment of SASS's impact alone was obtained.

In this paper, a variational formulation is used to assimilate the asynoptic SEASAT wind data with the NMC's synoptic surface pressure field over the North Atlantic Ocean for the 24 hours before, during and following the QE II storm's greatest intensity on September 10, 1978 1200 UT.

First, we describe the data sets and the methods used to convert that data to a stream function and relative vorticity estimates (Section 2). This is followed by the illustration of the apparent superiority of SASS winds in the storm region (Section 3), estimates (Section 2). This is followed by the illustration of the apparent superiority of SASS winds in the storm region (Section 3),

a description of the assimilation of the SASS data using a variational formulation (Section 4), and the adjusted surface pressure fields (Section 5). Finally Section 6 contains the summary and conclusions.

Data Base and Data Analysis Techniques

The data sets to be assimilated are the SEASAT Scatterometer-derived surface winds (SASS) and the National Meteorological Center (NMC) sea level atmospheric pressure field. The SASS winds have had the wind direction ambiguity removed by the technique described by Wurtele et al. (1982). There are approximately 15 days of data from September 6, 1978 0000 UT to September 10, 1978 1200 UT. The SASS data consists of the following: the time of the observation (in seconds from January 1, 1978), the location of the observation in latitude and longitude, the speed of the wind in ms^{-1} and the direction of the wind in degrees measured clockwise from north. The NMC pressure field is the result of the application of an objective analysis scheme of in situ observations. This field is then interpolated to several different grids. The grid, in our case, is a polar stereographic projection (Jenne, 1970), with a grid length of 381 km in each direction (at 60°N latitude). A square of 18 X 18 grid units was selected from this grid for study. This square corresponds to most of the North Atlantic Ocean (Figures 1). NMC uses any in situ observations within ± 3 hours of the analysis time as input to the objective analysis scheme (i.e. synoptic is defined as ± 3 hours). Consequently, the SASS wind data set is reduced to those observations within ± 3 hours of each NMC observation time as ± 3 hours). Consequently, the SASS wind data set is reduced to those observations within ± 3 hours of each NMC observation time

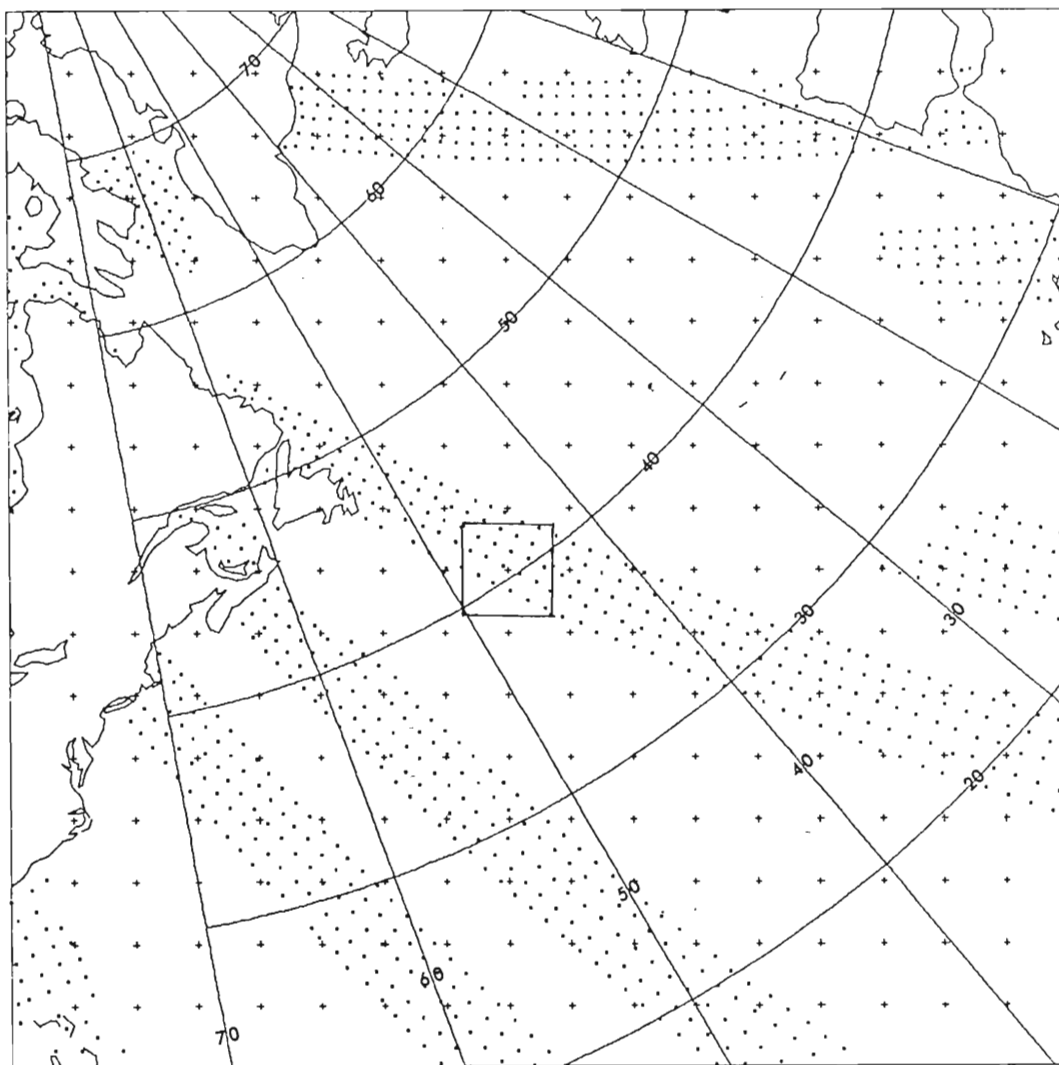


Fig.1a North Atlantic study region including SEASAT data points (dots) and NMC grid points (crosses). The square is a typical area from which SASS vorticity estimate is obtained for the center of the square. For September 9, 1978 1200 UT (OBS 7).
points (dots) and NMC grid points (crosses). The square is a typical area from which SASS vorticity estimate is obtained for the center of the square. For September 9, 1978 1200 UT (OBS 7).

OBS 8

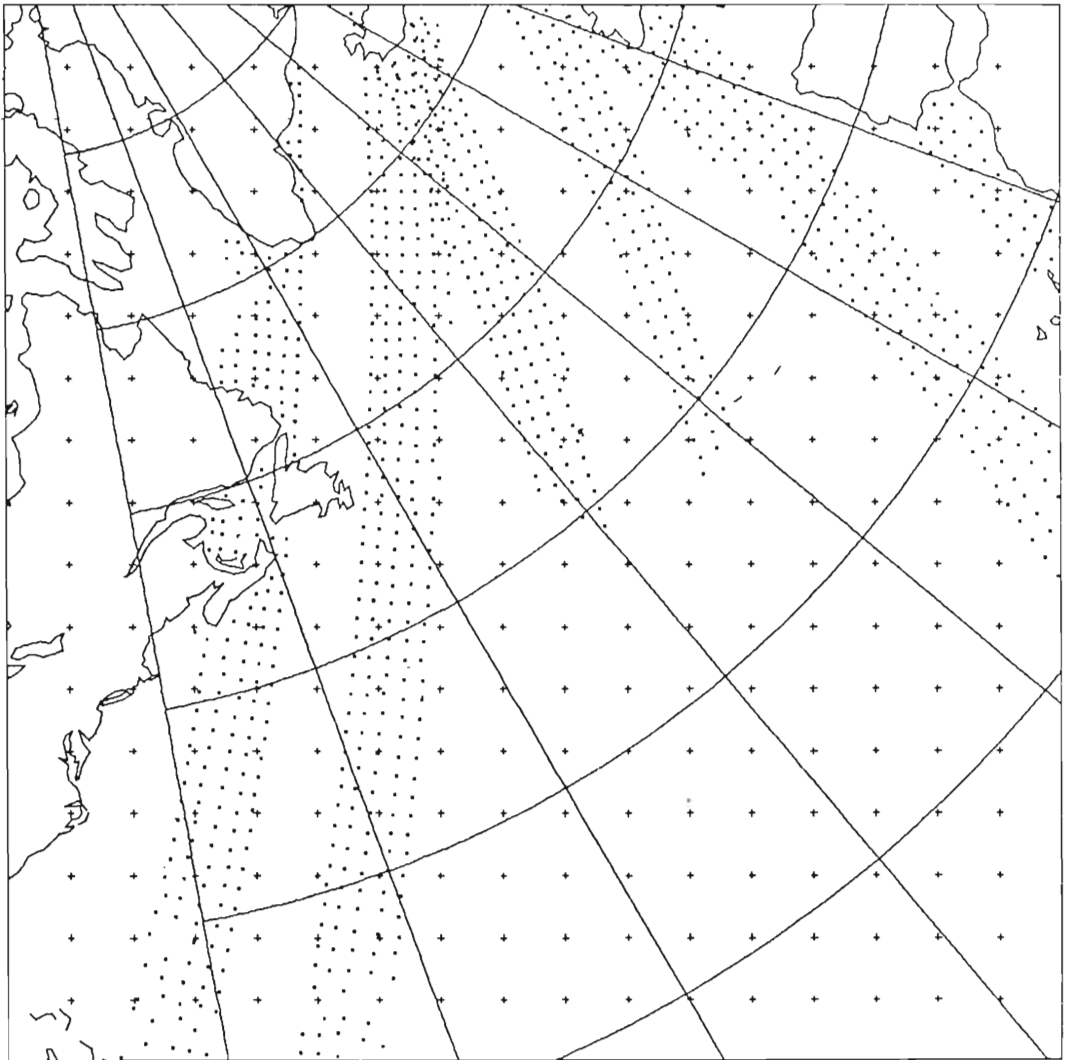


Fig.1b Same as Fig. 1a but for September 10, 1978 0000 UT (OBS 8).

Fig.1b Same as Fig. 1a but for September 10, 1978 0000 UT (OBS 8).

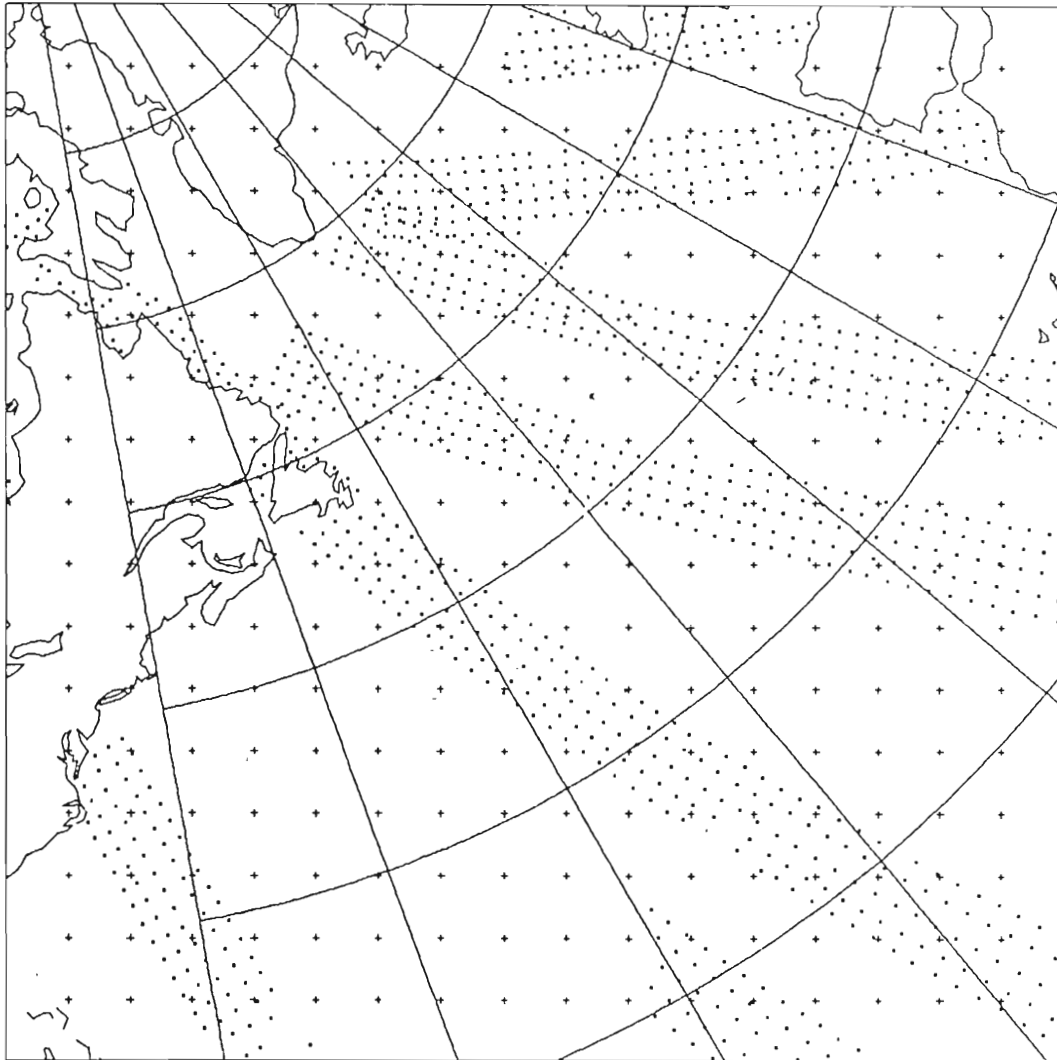


Fig.1c Same as Fig.1a but for September 10,1978 1200 UT (OBS 9).

Fig.1c Same as Fig.1a but for September 10,1978 1200 UT (OBS 9).

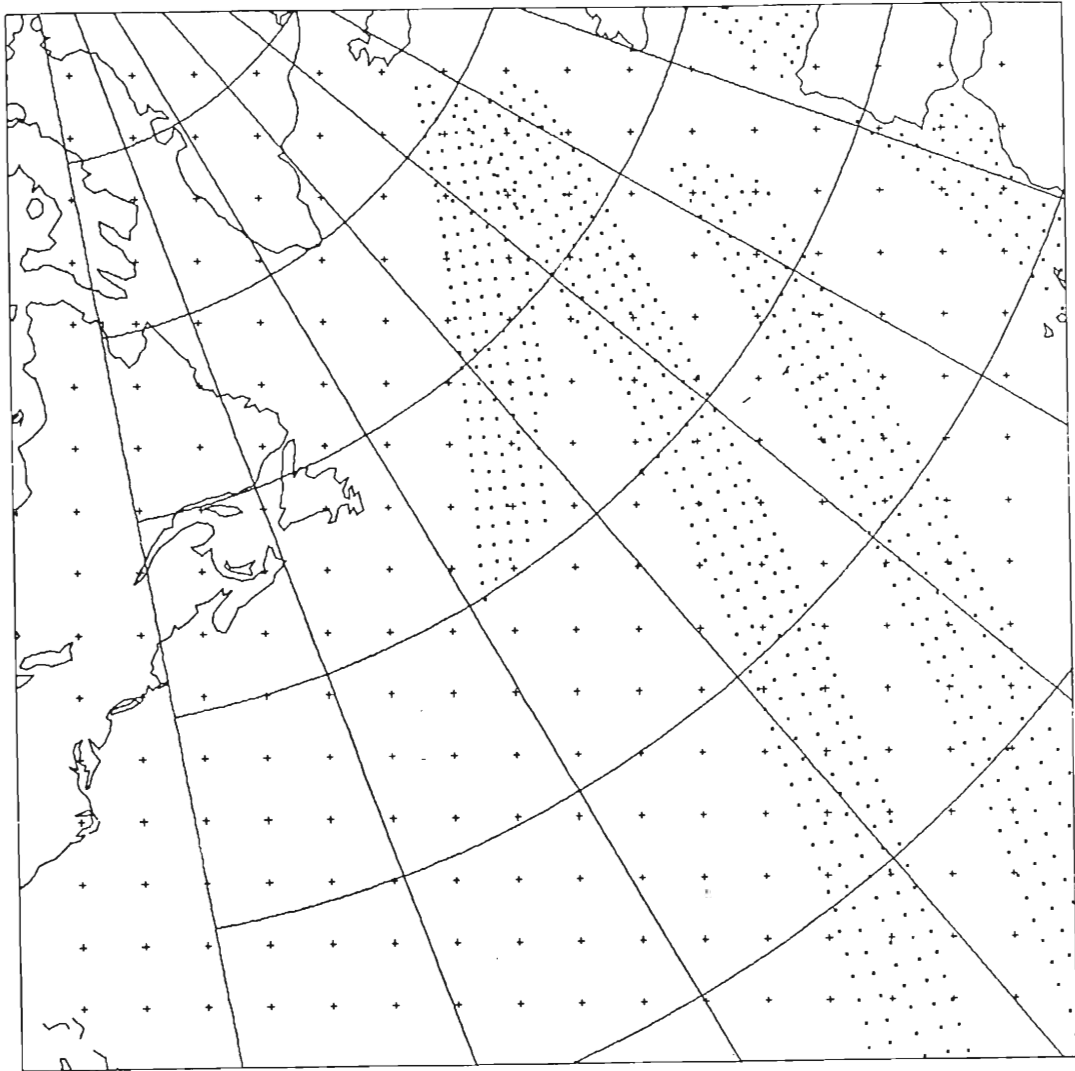


Fig.1d Same as Fig.1a but for September 11, 1978 0000 UT (OBS 10).

Fig.1d Same as Fig.1a but for September 11, 1978 0000 UT (OBS 10).

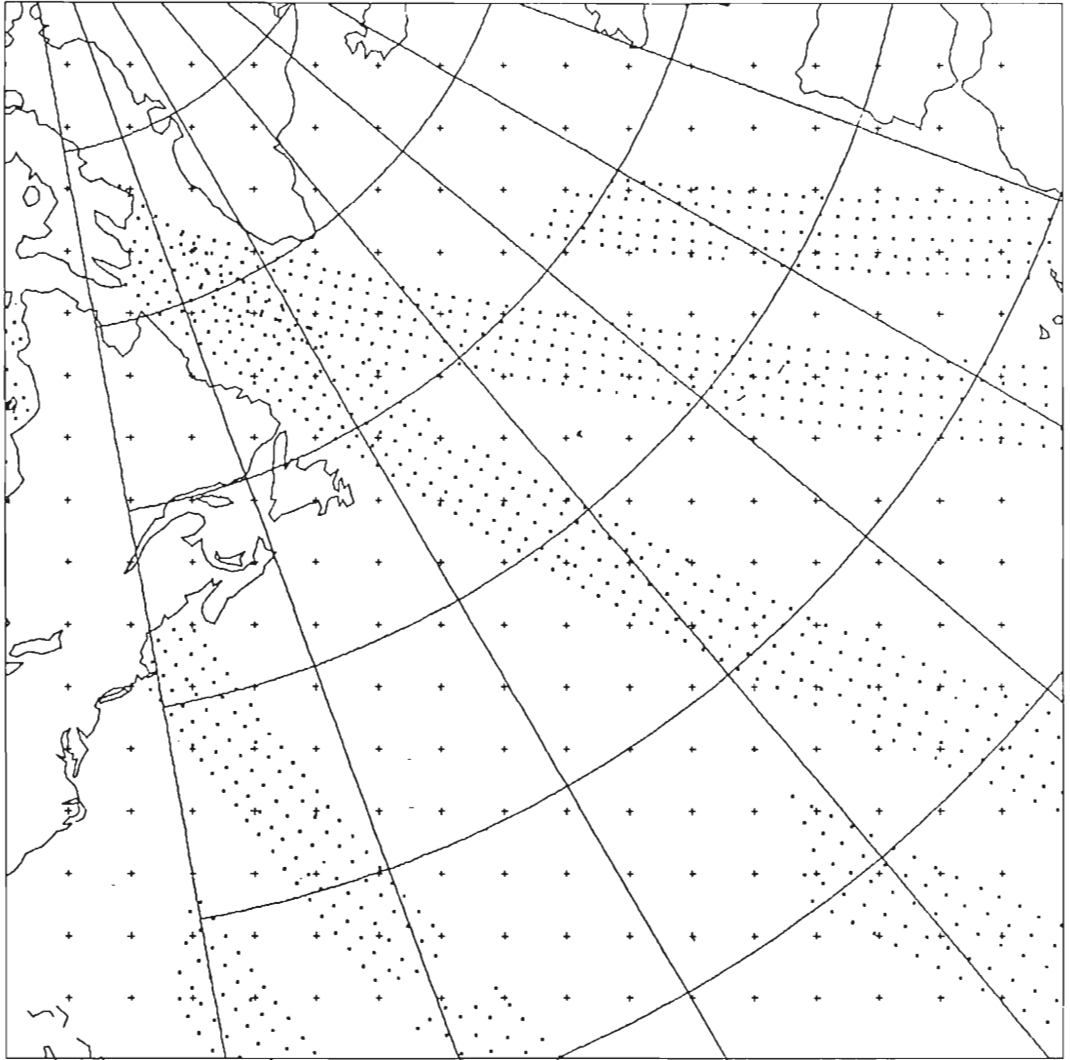


Fig.1e Same as Fig. 1a but for September 11, 1978 1200 UT (OBS 11).

Figure 1e Same as Fig. 1a but for September 11, 1978 1200 UT (OBS 11).

for all 15 days of de-aliased SASS wind data.

Because the NMC analyses are available every 12 hours, there are 30 NMC analyses corresponding to the 15 days of SASS data. This paper will be concerned with 5 of these analyses corresponding to the 48 hours before and including the QE II storm which occurred on September 11, 1978 (Figures 2.a-e). It should be stressed that the NMC analysis for OBS 9 had a low of 980 mb not 998 mb as in Figure 2c. The 998 mb value occurred due to smoothing when a fine resolution grid was interpolated to the coarser NMC octagonal grid. Figures 1.a-e illustrate the satellite data points for each of the 5 NMC analysis times. Chronologically, the SEASAT data runs from south to north and east to west.

Since we have two different data sets, one being surface pressure and the other being surface winds; a natural choice to relate these two data sets is relative vorticity. Using the SASS and NMC data sets described above, two relative vorticity estimates were calculated for each interior point of the NMC grid. It was necessary to calculate the two estimates by different techniques. This is due to the fact that, the NMC data are on a regular grid and the SASS data are irregularly spaced.

For the NMC data, a geostrophic stream function

$$Q_N(x,y) = \frac{P_N(x,y)}{\rho f}$$

was defined. It follows then that the relative vorticity at each point was defined. It follows then that the relative vorticity at each

ORIGINAL NMC P

OBS 7

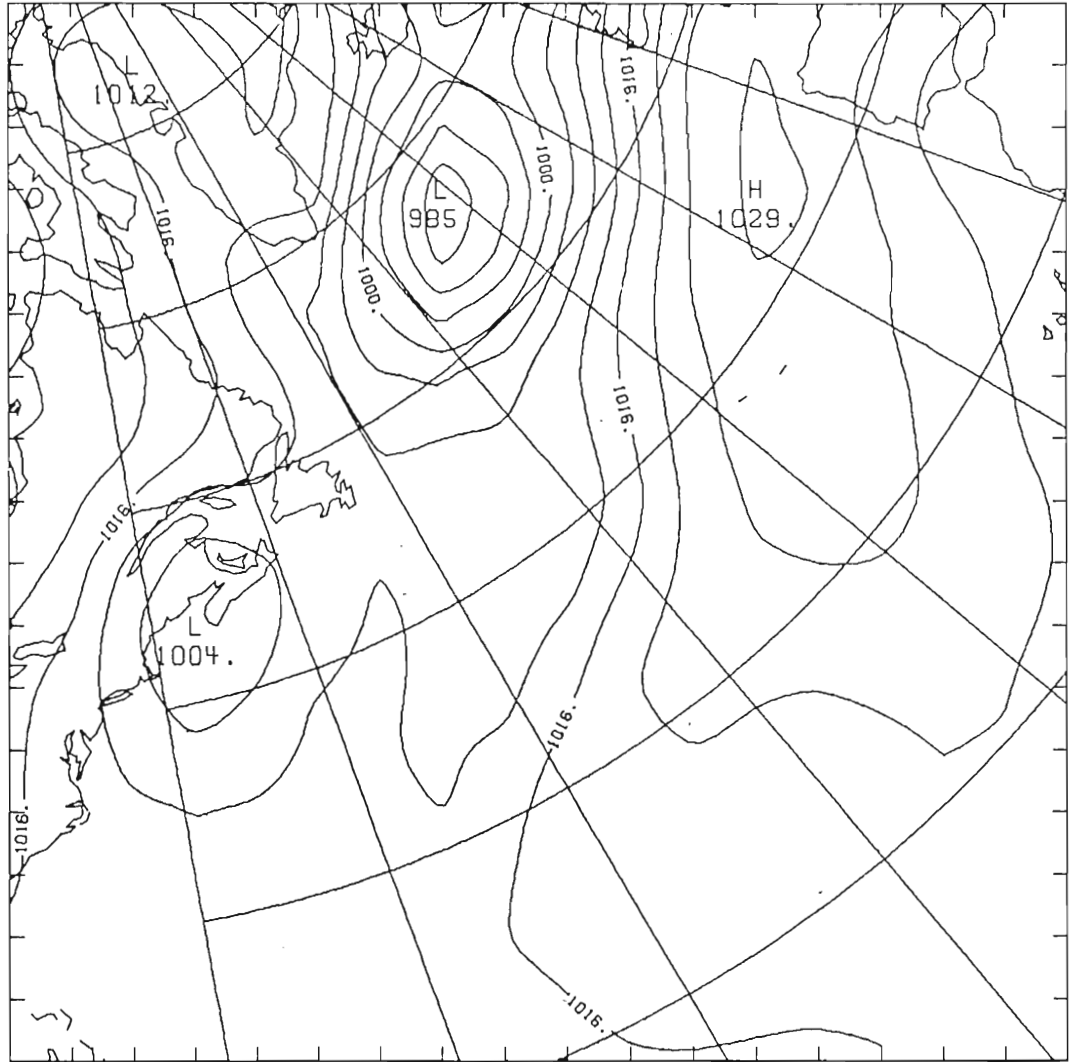


Fig.2a NMC surface analysis for Sept. 9, 1978 1200 UT (OBS 7).

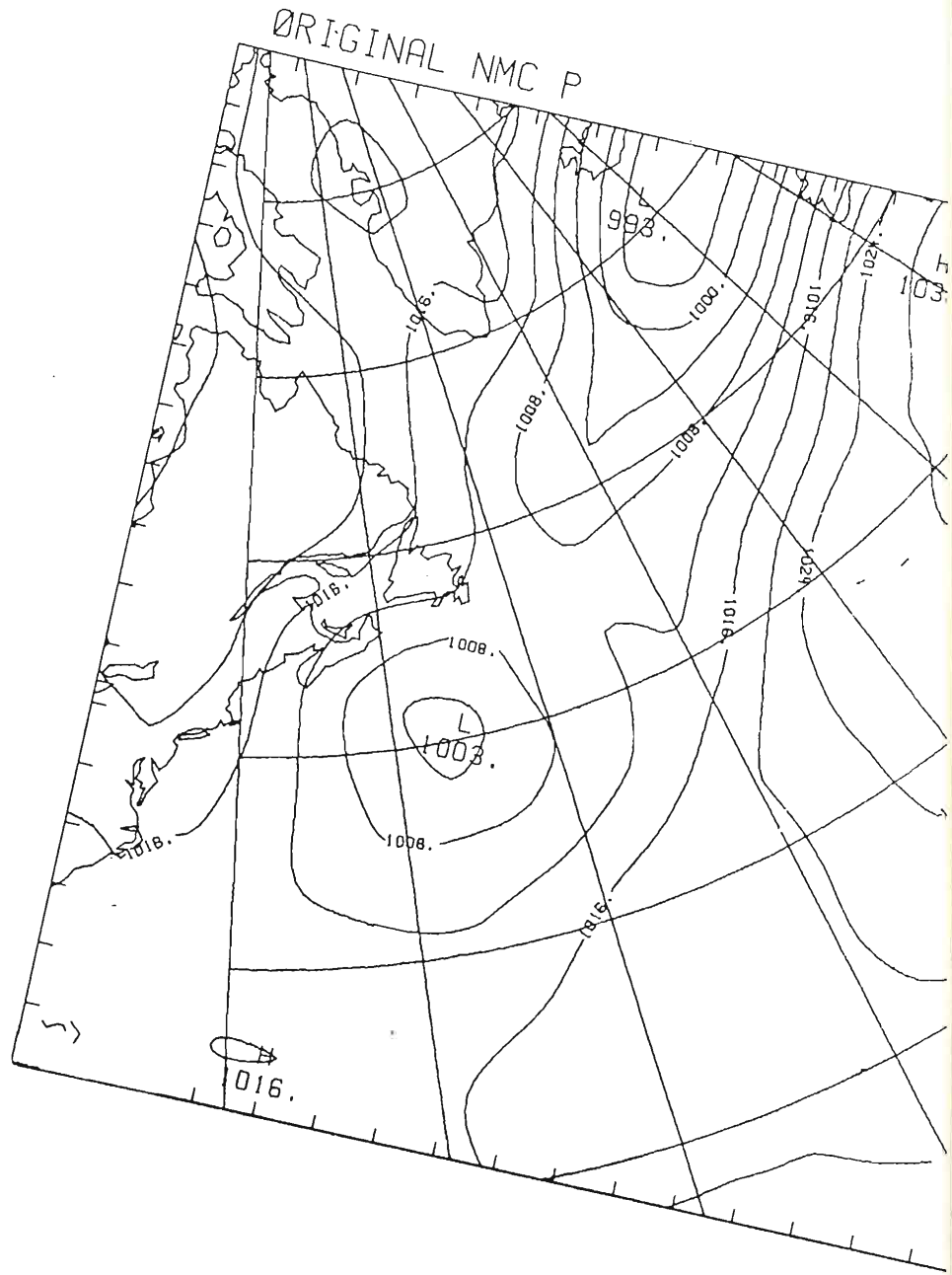


Fig.2b NMC surface analysis for Sept. 10, 1978 0000 UT (OBS 8)
- 0000 UT (OBS 8)

ORIGINAL NMC P

OBS 9

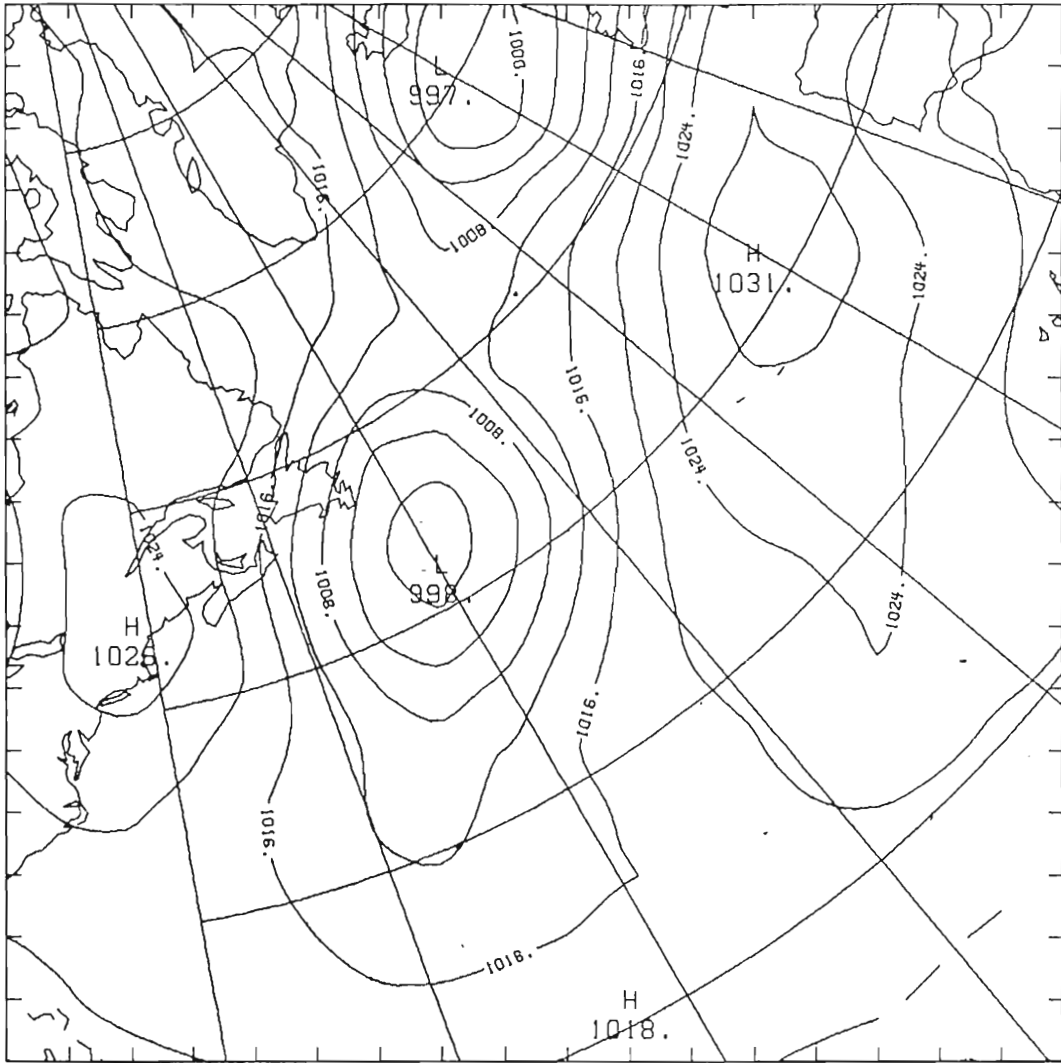


Fig.2c NMC surface analysis for Sept. 10, 1978 1200 UT (OBS 9)

ORIGINAL NMC P

OBS 10

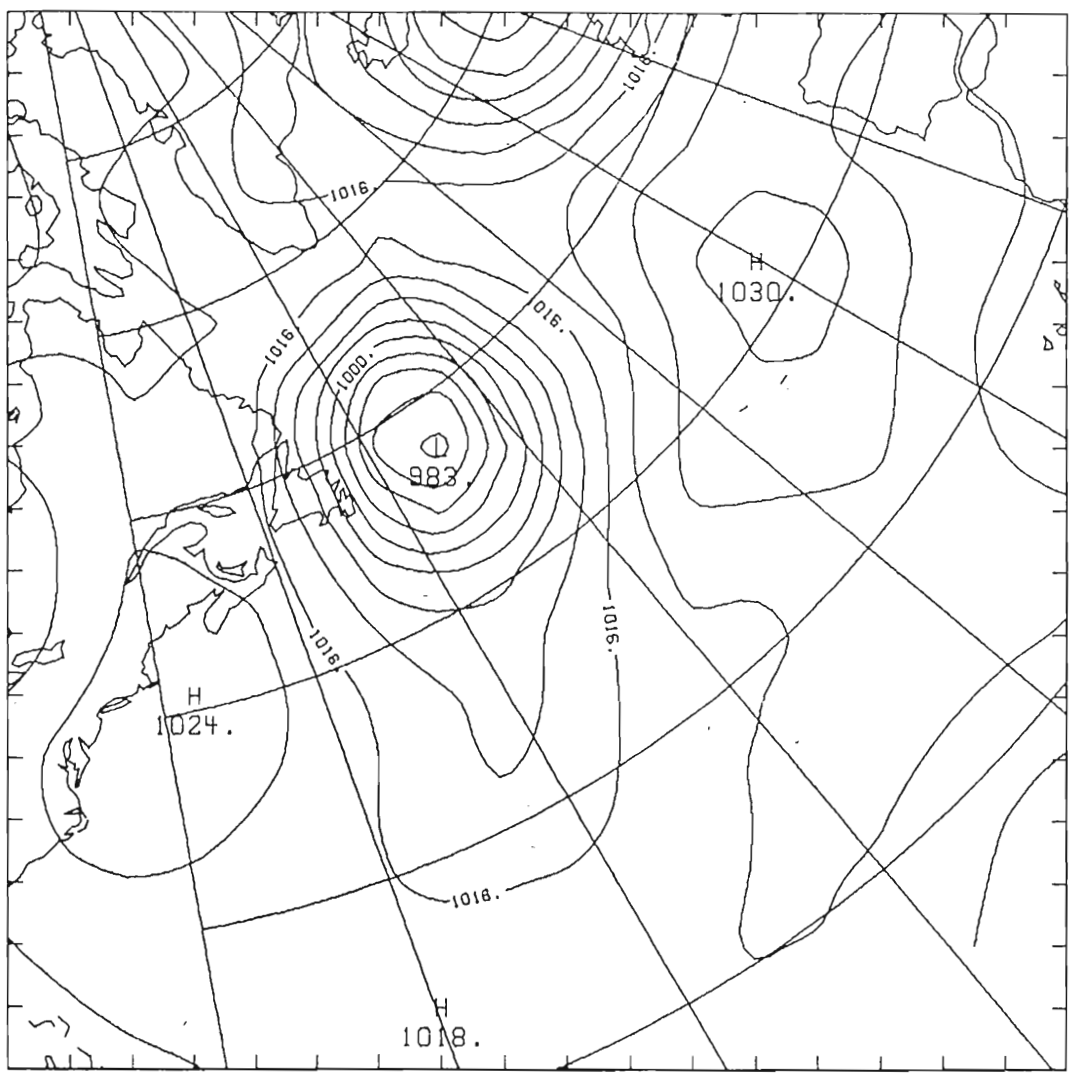


Fig.2d NMC surface analysis for Sept. 11, 1978 0000 UT (OBS 10)

ORIGINAL NMC P

OBS 11

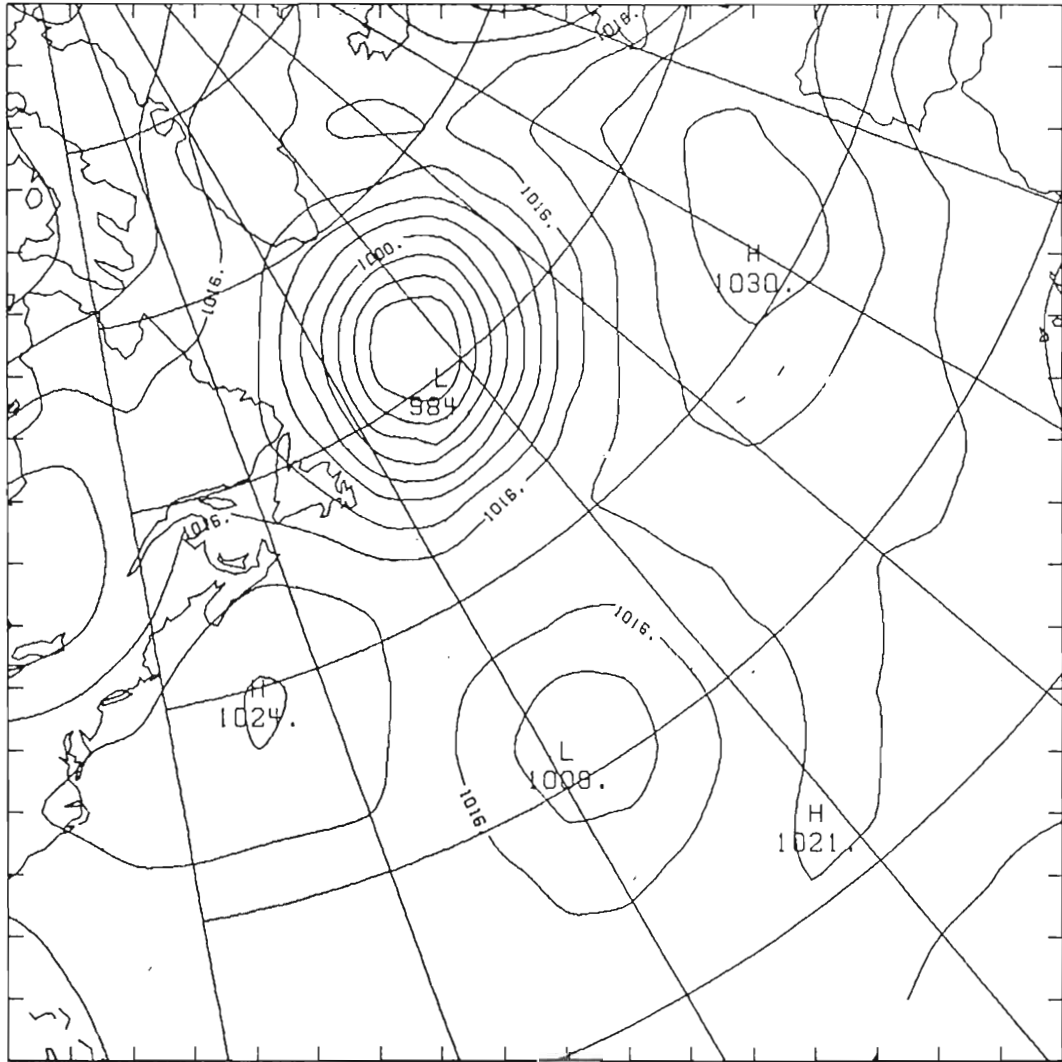


Fig.2e NMC surface analysis for Sept. 11, 1978 1200 UT (OBS 11)

NMC grid point is

$$\zeta_g(x,n) = \nabla^2 Q.$$

This was carried out using finite difference approximations.

Chapter 4 contains a complete description of this stream function and the relative vorticity estimates that result from it.

All calculations of the assimilation method are performed on the NMC grid, therefore an estimate of the relative vorticity using SASS winds is needed at each NMC grid point. In order to do this, a square surrounding each grid point was defined which binned the SASS data. One of these squares may contain 0 to about 40 SASS data points (Figure 1a). It is important to note that the satellite does not pass directly over every NMC grid point in the study region during the 6 hour time window.

These SASS data, then, define a region over which the vorticity must be calculated. From Stokes theorem,

$$\iint_A \vec{\zeta} \cdot \hat{n} dA = \int_C \vec{u} \cdot d\vec{r}$$

where C is the curve enclosing the surface A whose normal vector is \hat{n} . As δA becomes infinitesimally small, the mean value theorem permits the reduction of this equation to

$$\bar{\zeta} = \frac{\alpha \bar{u}}{\delta A}.$$

where $\bar{\zeta}$ is the average vorticity vector normal to the surface δA , \bar{u} is the average tangential velocity along the curve C which has a perimeter length, α (Pedlosky, 1982).

If we have the SASS data set of wind speed and direction located at a specific set of latitudes and longitudes, the numerator of the above expression can be calculated for each NMC grid point. Due to the complexity of finding the exact polygon whose perimeter would enclose all the SASS data points, a quadrilateral was chosen whose vertices are the SASS points nearest to the corners of the square. If fewer than four points exist, SASS vorticity is not calculated.

If we know the area of the region within a square for which there is SASS data and the location of each of those points and the magnitude and direction of the wind at those points, we can calculate the average relative vorticity normal to the surface of that region.

Comparison of Seasat Winds and Geostrophic Winds

One can easily find the zonal and meridional components of the geostrophic wind from the surface pressure field. The simplest method of determining the surface wind field from the geostrophic wind field is by a reduction-rotation model, in which the geostrophic wind is reduced by a constant factor and rotated counter-clockwise a constant number of degrees. This reduction-rotation method is a simple model of the decrease in velocity and turning of the boundary layer as the surface is approached.

In order to obtain a relationship between the SASS surface winds and the winds produced by the application of the reduction-rotation model to the NMC geostrophic winds, it was necessary to interpolate and transform from the NMC grid points to the SASS locations. The interpolation was biquadratic for the interior points and bilinear near the boundaries.

For each of the 5 NMC observation times, the optimum reduction and rotation constants were determined using a least squares formula minimizing

$$\psi = ||\vec{V}_s - R_1\vec{V}_g\exp(iR_2)||^2$$

where \vec{V}_g and \vec{V}_s are the geostrophic and SASS winds, respectively; R_1

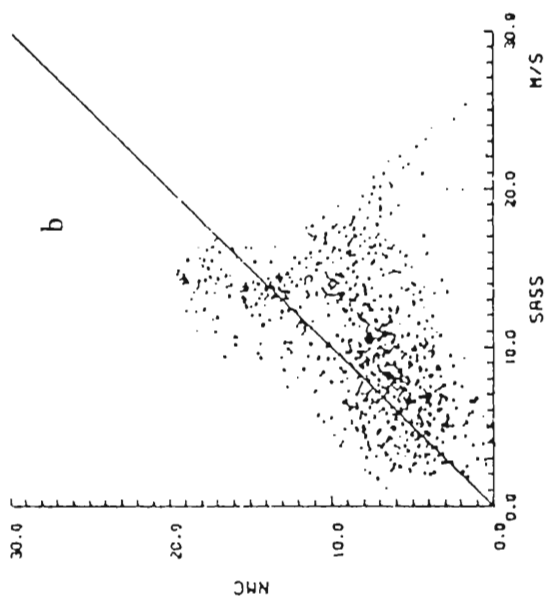
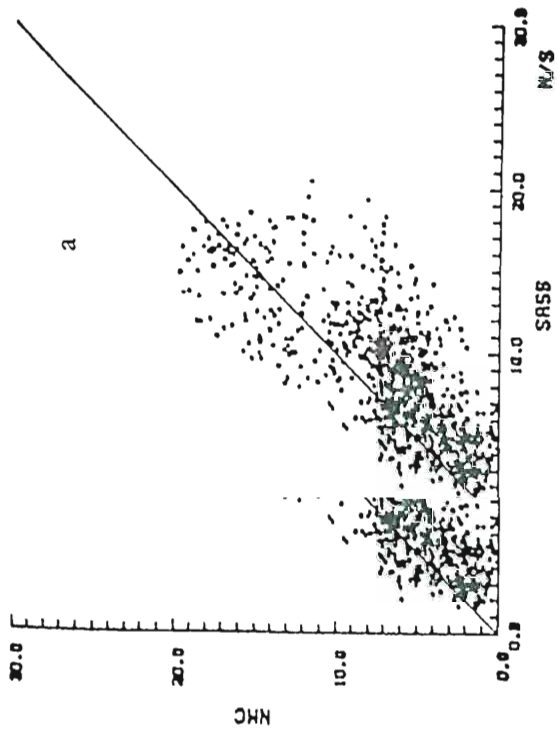
where \vec{V}_g and \vec{V}_s are the geostrophic and SASS winds, respectively; R_1 is the reduction constant and R_2 is the rotation constant.

The average reduction is 0.83 (± 0.09) and the average rotation is 27.6° (± 2.5) cyclonically. These values agree well with the observed reduction constants of 0.60 to 0.90 and rotation constants of 15° to 30° (Clarke and Hess, 1975). As is pointed out by Clarke and Hess (1975) and Hasse and Wagner (1971); the rotation and reduction factors vary with latitude and with the prevailing stability conditions.

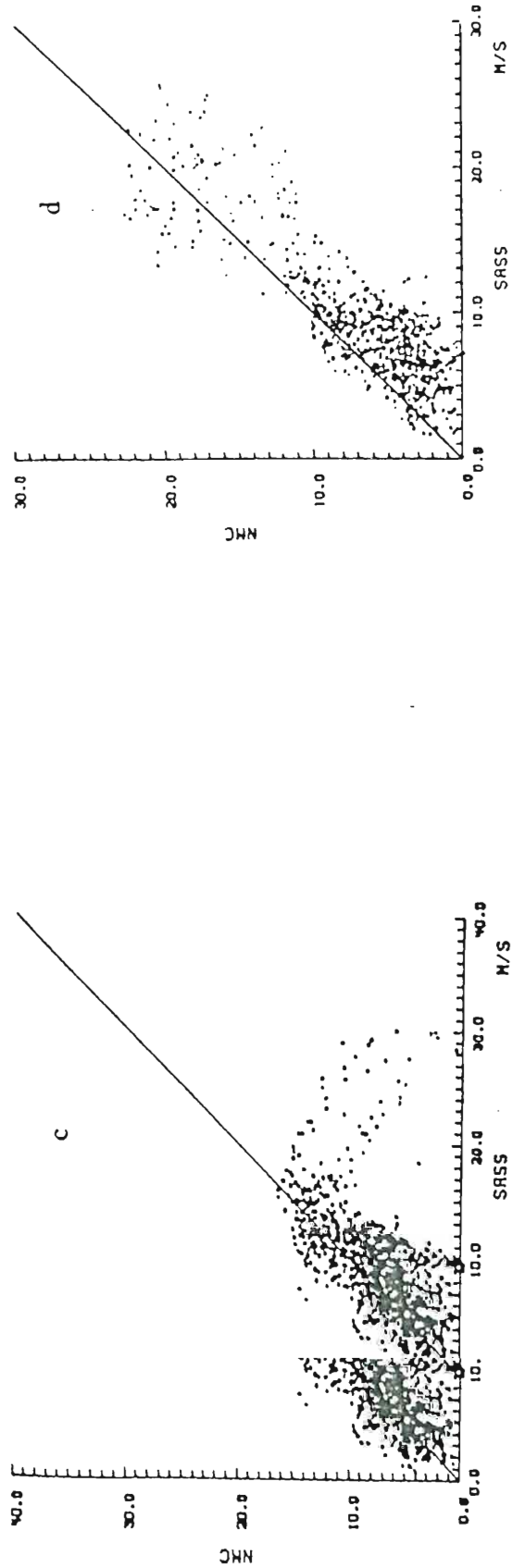
There are more sophisticated models, e.g. Brown (1978), available for producing surface winds from synoptic pressure fields (Overland, *et al.*, 1980). In a comparison with *in situ* surface winds, Thomas (1983) found the winds of Brown's model to have no significant improvement over the reduction-rotation model. Therefore, in order to demonstrate our assimilation technique, the reduction-rotation method should be adequate.

Using the reduction and rotation constants obtained by the least-squares technique, scatter plots were made of the Seasat winds versus the reduced-rotated NMC geostrophic winds for each of the 5 analysis times from September 9, 1978 1200 UT to September 11, 1978 1200 UT. Plots are made for the entire North Atlantic region under study for vector magnitude (Figures 3.a-e) as well as for subsets of this region whose boundaries have been chosen so as to include only the QE II storm (or its precursor) (Figures 4.a-e).

Although the reduction-rotation factors have been determined to minimize the error between the SASS surface winds and the pressure-
minimize the error between the SASS surface winds and the pressure-



F Fig. 3a-b SASS wind speed vs. reduced-rotated geostrophic winds for entire 6 hour time window and entire study area.
 (a) for OBS 7, $r^2 = 0.53$ (b) for OBS 8, $r^2 = 0.21$



F Fig.3c-d SASS wind speed vs. reduced-rotated geostrophic winds for entire 6 hour time window and entire study area. Note different scale sizes. (c) for OBS 9, $r^2 = 0.31$ (d) for OBS 10, $r^2 = 0.74$

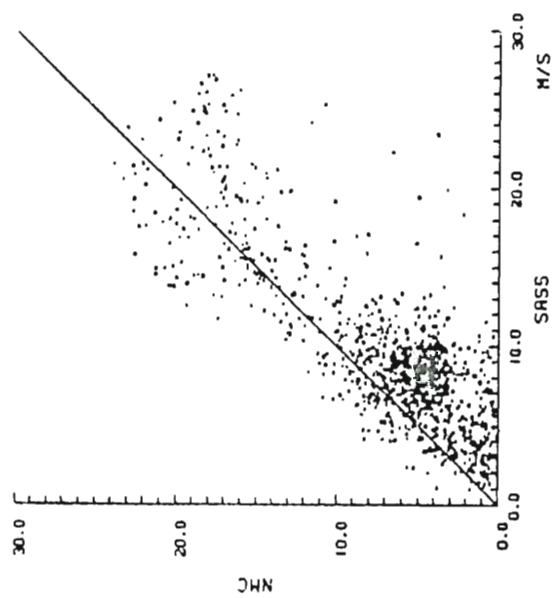


Fig.3e SASS wind speed vs. reduced-rotated geostrophic winds for entire 6 hour time window and entire study area. (e) for OBS 11, $r^2 = 0.67$

field-derived winds, it is apparent from Figure 3 that the SASS winds are higher than the NMC winds at lower wind speeds ($<10\text{ms}^{-1}$). This is in agreement with the generally accepted observation that SASS overestimates low wind speeds ($<10\text{ms}^{-1}$) (Jones, et al., 1982). The companion observation is that SASS underestimates high winds ($>\approx 20\text{ms}^{-1}$) (Jones, et al., 1982).

It is important to note that in the JASIN study of Jones, et al., (1982) the SASS winds were compared with very reliable and accurate ground truth wind vectors at precise locations. In this study, the geostrophically-derived surface winds are certainly not as accurate as the SASS winds due to numerous approximations. Pierson (1981) made similar scatter-plot comparisons to those presented here using conventional ship data consisting of anemometer measurements and Beaufort estimates of the surface winds taken during the QE II storm, which are actually time averages of the wind. He concluded that the conventional wind estimates were on average too low for high wind speeds. The scatter plots of Figures 4.a-e can, similarly, be interpreted as evidence that the geostrophic winds provide too low an estimate for the surface wind speed for high wind speeds. If we accept the fact that the NMC surface pressure analysis for at least two of these analysis times have too high a pressure in the storm region, it follows that the geostrophic wind speeds corresponding to the storm would be expected to be too small.

geostrophic wind speeds corresponding to the storm would be expected to be too small.

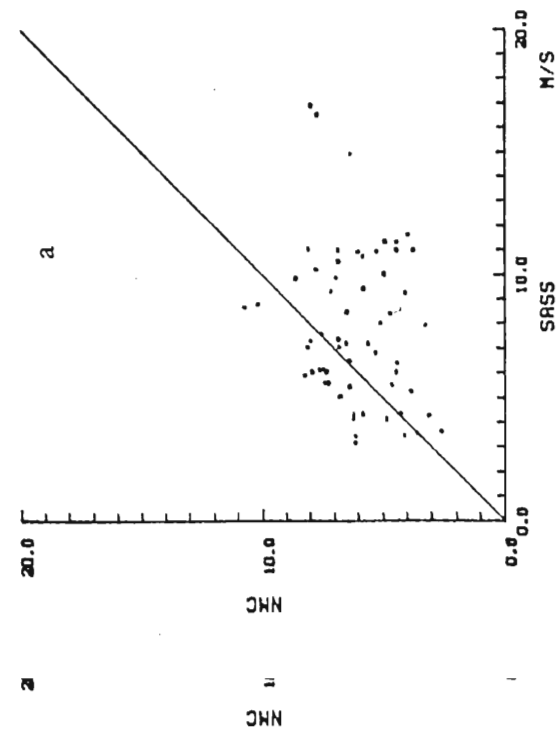
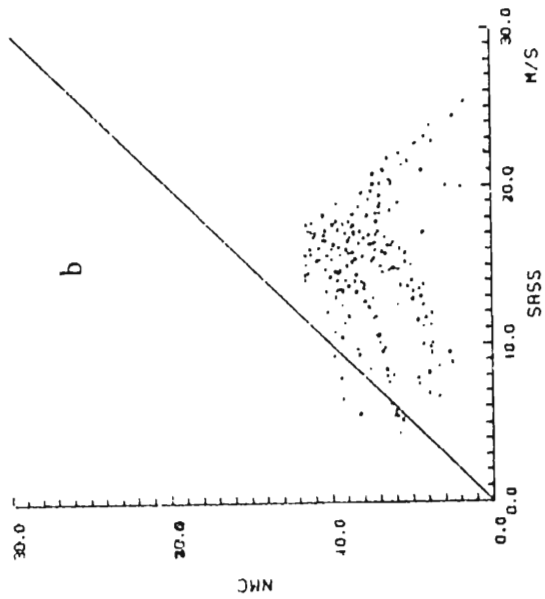


Fig.4a-b Same as Fig.3 but for a sub-region encompassing only the storm.
 (a) for OBS 7, $r^2 = 0.04$
 (b) for OBS 8, $r^2 = 0.01$
 Note different size scales.

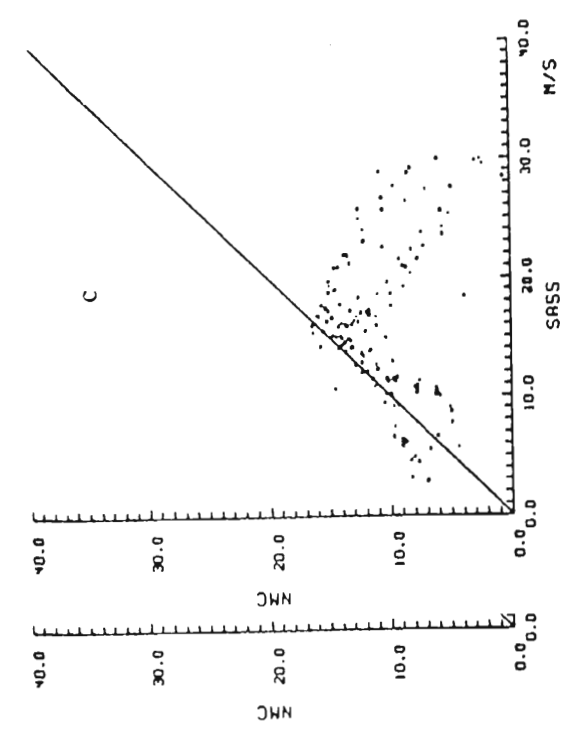
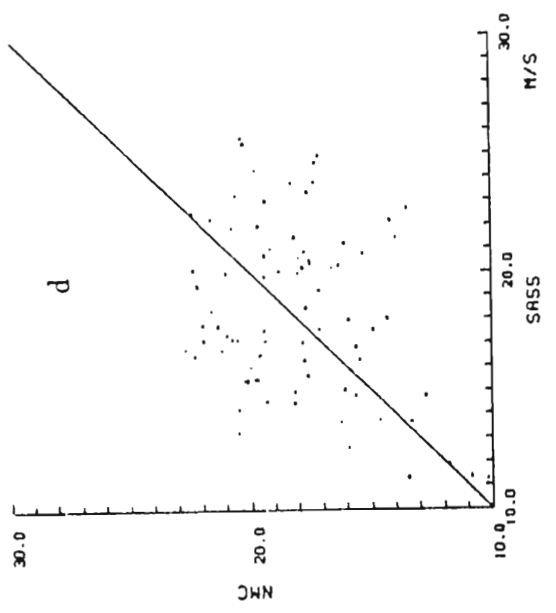


Fig.4c-d Same as Fig.3 but for a sub-region encompassing only the storm.
 (c) for OBS 9, $r^2 = 0.00$
 (d) for OBS 10, $r^2 = 0.08$
 Note different scale sizes.

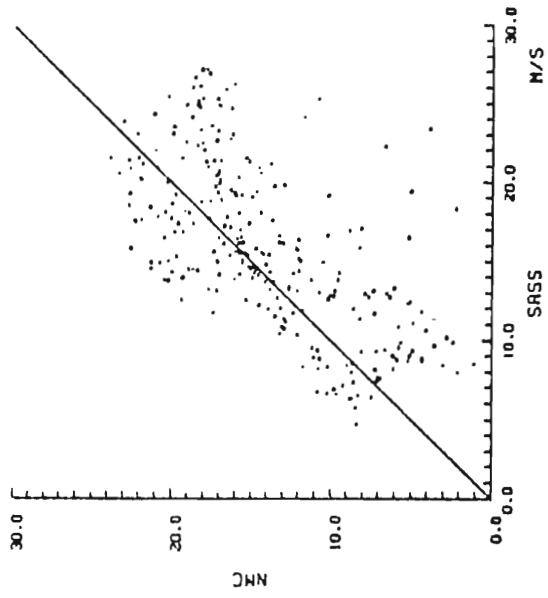


Fig.4e Same as Fig.3 but for a sub-region encompassing only the storm.
(e) for OBS 11, $r^2 = 0.42$

Assimilation Technique by a Variational Principle

Satellite data is asynoptic and therefore, presents a problem if we try to assimilate them with conventional meteorological data sets. In this section, a technique is described which enables this assimilation using a vorticity estimate from each data set at every point on a grid. As is pointed out by Pierson (1983), the ship reports and data buoys used to compute the wind field and, subsequently, the pressure field for the NMC surface pressure analysis introduce mesoscale perturbations into the synoptic scale field due to their short averaging times. Pierson's (1983) concept of "equivalent averaging time", which relates temporal averaging to spatial averaging, states that the equivalent time it takes for an eddy to be advected by the mean wind over a distance D is given by

$$T_e = D/\bar{u}.$$

A scatterometer wind field with a resolution of approximately 100 km and a mean wind of 10 ms^{-1} would be equivalent to an averaging time of about 2.8 hours. Therefore, scatterometer winds are a more accurate representation of the synoptic scale wind field than the ship and data buoy winds used by NMC. The SASS time is considered to be synoptic for any time within $\pm T_e/2$. Therefore, if, for example, the SASS time is 1.3 hours from the NMC analysis time, it is given a weight of 1.0. Since the SASS winds data set was reduced at the the SASS time is 1.3 hours from the NMC analysis time, it is given a weight of 1.0. Since the SASS winds data set was reduced at the outset to include only those winds ± 3.0 hours from the NMC analysis

time, the smallest weight given to any SASS vorticity would be

$$F_{ij} = 1.0 - 1.6/3.0 = 0.47.$$

Most weights, therefore, will be greater than 0.50.

We still have the problem of asynoptic sampling since the time at which the scatterometer spatial averaging is done differs from the NMC analysis time. In order to insert this data into the NMC surface pressure field, the SEASAT data is weighted with respect to time. This is in contrast to the NMC procedure of considering all the ship and data buoy reports occurring with the ± 3.0 hour window as being synoptic for a given analysis time. Improvements in the overall synoptic surface pressure field might be possible by assimilating the SEASAT data using a method that weights that data with respect to its nearness to the NMC analysis time. Due to the irregular coverage by the satellite, a smooth surface pressure field would be difficult, if not impossible, to achieve if only satellite data were used to obtain the synoptic pressure field. Thus, we need a weighting technique that allows the use of both the original NMC pressure field and the SASS data.

From conventional NMC pressure analyses, P_N , one can construct a stream function

$$Q_N(x,y) = \frac{1}{\rho f} P_N(x,y) \quad (1)$$

where N denotes NMC and ρ is density at the surface and f is the Coriolis parameter. These fields also vary with time, but the time dependence is parametric and not crucial to the present diagnostic Coriolis parameter. These fields also vary with time, but the time dependence is parametric and not crucial to the present diagnostic approach. From this stream function, a geostrophic relative

vorticity can be calculated

$$\zeta_g(x,y) = \frac{\partial v}{\partial x} - \frac{\partial u}{\partial y} = \frac{\partial^2 Q_N}{\partial x^2} + \frac{\partial^2 Q_N}{\partial y^2}$$

where the subscript 'g' refers to the geostrophic nature of this vorticity field. In practice, a finite difference approximation is used

$$\begin{aligned} \zeta_g(x_i, y_j) = \zeta_{gij} = & (Q_{i+1,j} + Q_{i-1,j} - 2Q_{ij})/\Delta x^2 \\ & + (Q_{i,j+1} + Q_{i,j-1} - 2Q_{ij})/\Delta y^2 \end{aligned} \quad (2)$$

The Seasat data provide another vorticity field, as described in Chapter 2,

$$\zeta_{sij} = \frac{\bar{u}_i \bar{v}_j}{\delta A}$$

where the subscript 's' refers to the satellite origin of this second vorticity field.

The weighting function referred to above, is

$$F_{ij} = 1.0 - \frac{|(\text{SASS time}) - (\text{NMC time})|}{3.0 \text{ hours}} \quad (3)$$

where NMC time is the time for which the analysis was made and SASS time is the average ± 1.4 hours of the times of the 4 SASS data points used in the calculation of the relative vorticity field. If the SASS time differs from the NMC time by more than 3 hours, F_{ij} is taken equal to zero. With this factor, a weighted vorticity field can be constructed by interpolation

$$\zeta_{dij} = F_{ij}\zeta_{sij} + (1 - F_{ij})\zeta_{gij} \quad (4)$$

If the NMC analysis time equals the satellite observation time, $F_{ij} = 1.0$ and the new vorticity is taken to be the instantaneous satellite vorticity, which is naturally thought to be an improvement over the geostrophic estimate. If a satellite observation is available during the 6 hour (± 3.0 hours) time window, the new vorticity relies on both the SASS and geostrophic estimates, provided $F_{ij} < 1.0$. Finally, if no satellite information is available within the time window, the vorticity is simply the geostrophic estimate.

With this formulation, one can expect a lack of horizontal smoothness. For example, consider two neighboring grid points such that, at a particular time, one is covered by a satellite swath and the other is not. One point is assigned the satellite vorticity while the neighbor is assigned the geostrophic vorticity. The composite vorticity field is expected to be noisy. We need to introduce a smoothing operator to remove the noise.

In order to assimilate the data from NMC and SASS, we propose a variational formulation. In general we can construct a difference functional, S ,

$$S(Q_{ij}, \zeta_{ij}, \lambda_{ij}) = \sum_{ij} \lambda_{ij} H_{ij} + \sum_{ij} \frac{K_z}{2} v_{ij}^2 + \sum_{ij} \frac{K_E}{2} G(Q_{ij}) \quad (5)$$

This is the method of strong constraints (Sasaki, 1970). The first term is our model, H_{ij} , at each grid point multiplied by a Lagrangian multiplier λ_{ij} . In this study, our model is

$$H_{ij} = \nabla^2 Q_{ij} - \zeta_{ij} \quad (6)$$

Lagrangian multiplier λ_{ij} . In this study, our model is

$$H_{ij} = \nabla^2 Q_{ij} - \zeta_{ij} \quad (6)$$

Both Q_{ij} and ζ_{ij} will be determined; i.e., they will be the best pressure field and vorticity field which can satisfy the constraints. The last two terms are the constraints.

The V_{ij} are the data misfits or, in this case, they might be called vorticity discrepancies.

$$V_{ij} = \zeta_{ij} - [F_{ij}\zeta_{sij} + (1 - F_{ij})\zeta_{gij}] = \zeta_{ij} - \zeta_{dij} \quad (7)$$

If the weighted vorticities from the data exactly agree with the variational solution, then V_{ij} will be zero. The symbol, K_ζ , is a Gauss precision modulus. It is a free parameter in the solution. It may be chosen to be a function of space. Usually it depends inversely on the error variance of each data point. In our study it will be taken as a constant. This will be discussed later.

The last term is a "penalty function". In general, G is some quadratic function of the pressure field. In effect it is the smoothing operator necessary for horizontal blending of the data fields. The parameter, K_E , is another coefficient to be discussed later. It should be noted that larger K_E will introduce more horizontal smoothing.

There are many choices of penalty functions. We choose to require the kinetic energy to be minimized where

$$G(Q_{ij}) = \frac{1}{2}(u^2 + v^2) = \frac{1}{2}\nabla Q_{ij} \cdot \nabla Q_{ij} \quad (8)$$

Many other choices are possible but this one leads to tractable

Many other choices are possible but this one leads to tractable

equations to solve.

If we find a minimum of S , in essence we are solving the problem: Find Q_{ij} and ζ_{ij} on the grid subject to the condition that the data misfits are as small as possible and the constraint that the average kinetic energy is a minimum and the adjusted pressure field and vorticity satisfy the model. We have two free parameters, K_ζ and K_E , but as will be shown we really only have one free parameter, the ratio $K = K_E/K_\zeta$.

The problem is now to minimize the residuals by minimizing the function S . Optimization of S is obtained when the variations with respect to its variables, λ_{ij} , ζ_{ij} , and Q_{ij} , vanish. We find

$$\frac{\partial S}{\partial \lambda_{ij}} = H_{ij} = 0 \quad (9)$$

$$\frac{\partial S}{\partial \zeta_{ij}} = K_\zeta V_{ij} - \lambda_{ij} = 0 \quad (10)$$

$$\begin{aligned} \frac{\partial S}{\partial Q_{ij}} = & \frac{\lambda_{i+1,j} + \lambda_{i-1,j} - 2\lambda_{ij} +}{\Delta x^2} + \\ & \frac{\lambda_{ij+1} + \lambda_{ij-1} - 2\lambda_{ij} - K_E [\frac{Q_{i+1,j} + Q_{i-1,j} - 2Q_{ij} +}{\Delta x^2} + }{\Delta y^2} \\ & \frac{Q_{ij+1} + Q_{ij-1} - 2Q_{ij}]}{\Delta y^2} = 0 \end{aligned} \quad (11)$$

Equation (11) yields two results with respect to arbitrary but small

variations, δQ , of Q :

(a) Arbitrariness of δQ inside the domain implying

$$\nabla^2 \lambda = K_E \nabla^2 Q$$

(b) Arbitrariness of normal derivative of δQ on the boundary

implying

$$\lambda = 0 \text{ on boundary.}$$

Therefore, the most general solution to equation (11) is

$$\lambda_{ij} = K_E(Q_{ij} - Q_{0ij}) \quad (12)$$

where $K_E Q_{0ij}$ is any solution to the homogeneous problem for λ_{ij}

($\nabla^2 \lambda_{ij} = 0$) and $K_E Q_{ij}$ is a particular solution to the

non-homogeneous problem. Q_0 thus satisfies

$$\nabla^2 Q_0 = 0,$$

and $\lambda = 0$ on boundary yields.

$$Q_0 = Q_b \text{ on the boundary}$$

where Q_b is the boundary condition for Q .

From (7), equation (10) can be written as

$$K\zeta [\zeta_{ij} - [F_{ij}\zeta_{sij} + (1 - F_{ij})\zeta_{gij}]] = \lambda_{ij}. \quad (13)$$

Equations (12) and (13) imply

$$\zeta_{ij} = F_{ij}\zeta_{sij} + (1 - F_{ij})\zeta_{gij} + K(Q_{ij} - Q_{0ij}). \quad (14)$$

In order to obtain new estimates of the pressure field, (14)

is substituted into (9) using (6) to obtain

In order to obtain new estimates of the pressure field, (14)

is substituted into (9) using (6) to obtain

$$\frac{Q_{i+1j} + Q_{i-1j} - 2Q_{ij}}{\Delta x^2} + \frac{Q_{ij+1} + Q_{ij-1} - 2Q_{ij}}{\Delta y^2} - K(Q_{ij} - Q_{oij})$$

$$= F_{ij}\zeta_{sij} + (1 - F_{ij})\zeta_{gij}. \quad (15)$$

Given the function Q_0 and a value for K ; (15) can be solved numerically resulting in a new stream function field and thus new pressure and vorticity fields. The numerical method used is successive overrelaxation; with the field, Q_N , given in (1) as an initial guess.

In equation (14), the ratio, $K = K_E/K_\zeta$ can be thought of as a "tuning" factor; since it may be chosen so as to provide a balance between the kinetic energy constraint (8) and the constraint which minimizes the error in the modified vorticity (7).

We can explore the ratio of the penalty function to the data misfit by noting that from (5) and (14) we have

$$V_{ij} = K(Q_{ij} - Q_{oij}). \quad (16)$$

Substituting (16) into (5), the first term of (5) becomes

$$\sum_{ij} \frac{1}{2} K(Q_{ij} - Q_{oij})^2. \quad (17)$$

The ratio of the third term in (5) to the new first term of (5) (i.e. (17)) is:

$$R(K) = \frac{\sum_{ij} (\nabla Q \cdot \nabla Q)_{ij}}{\sum_{ij} K(Q_{ij} - Q_{oij})^2}.$$

$$\frac{\sum_{ij} (\nabla Q \cdot \nabla Q)_{ij}}{\sum_{ij} K(Q_{ij} - Q_{oij})^2}.$$

This is the ratio of the penalty function to the data misfit.

When $R(K)$ is 1.0, there is an exact balance between the two constraints mentioned above. If R is smaller than 1.0, more variation in the resultant Q field is allowed since kinetic energy is not minimized as much. Conversely, if R is greater than 1.0, more smoothing is done to the Q field.

For each of the 5 observation times in this study (OBS 7-11), the value of K which produces an R that is equal to 1.0 was found. This "tuning" value, K , was always between 1.0×10^{-12} and 2.0×10^{-12} . However, in practice, it was found that a tuning factor in this range resulted in a slightly smoother field than visually desired. Therefore, a value of R of about 1/3 was normally chosen when carrying out the numerical solution of (15). This resulted in retention of more variability in the field and consequently prevented smoothing out physical features which were known to be physically correct.

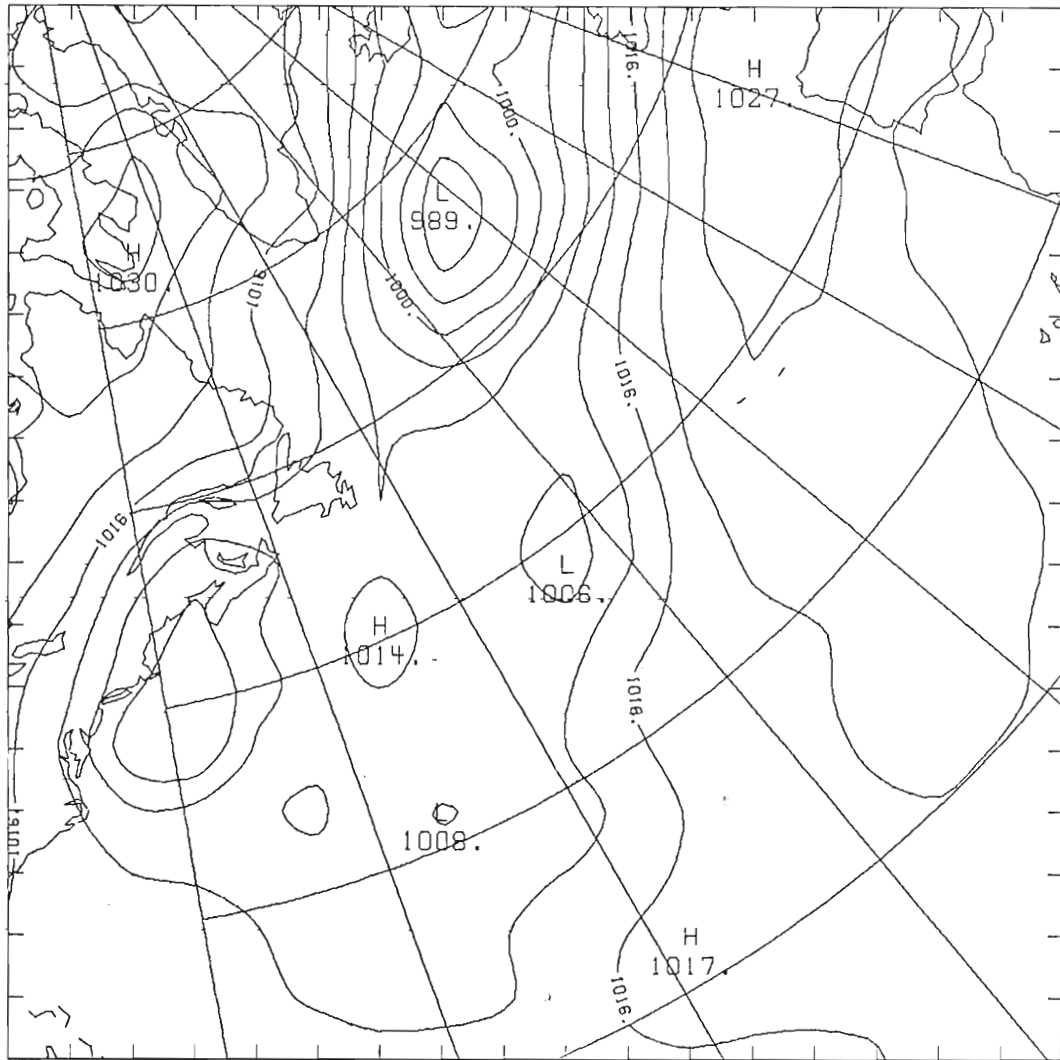
Results of Assimilation of SEASAT Winds

The concensus among the meteorological community, regarding the QE II storm, is that the NMC analysis for September 10, 1978 1200 UT (OBS 9) (Figure 2.c) was in error both in locating the storm center and in estimating its intensity. The central pressure of the storm is 980 mb located about 42°N 50°W according to NMC. Gyakum (1983) subjectively assimilated SEASAT winds along with the barograph tracing of the Euroliner and extrapolated to the storm center producing an estimated central pressure of 945 mb.

As mentioned above, the SASS winds are treated as being synoptic for a time window of ± 1.4 hours centered on the actual time of the SASS observation. Recalling that the SASS data were reduced to only those in the ± 3.0 hour time window centered on the NMC analysis time, it becomes evident that the smallest possible weighting for a SASS relative vorticity estimate is 0.47. Consequently, the average weighting is about 0.75 to 0.80. Thus, by using the weighted SASS vorticities, one is already giving a majority of them more weight than that given to the geostrophic vorticity estimates. In addition, the adjusted pressure fields using weighted SASS vorticities (Figure 5a-e) do not differ very much from their counterparts which use substitution of SASS vorticities for their counterparts which use substitution of SASS vorticities for

ADJUSTED P

ØBS 7



ADJUSTED P

OBS 8

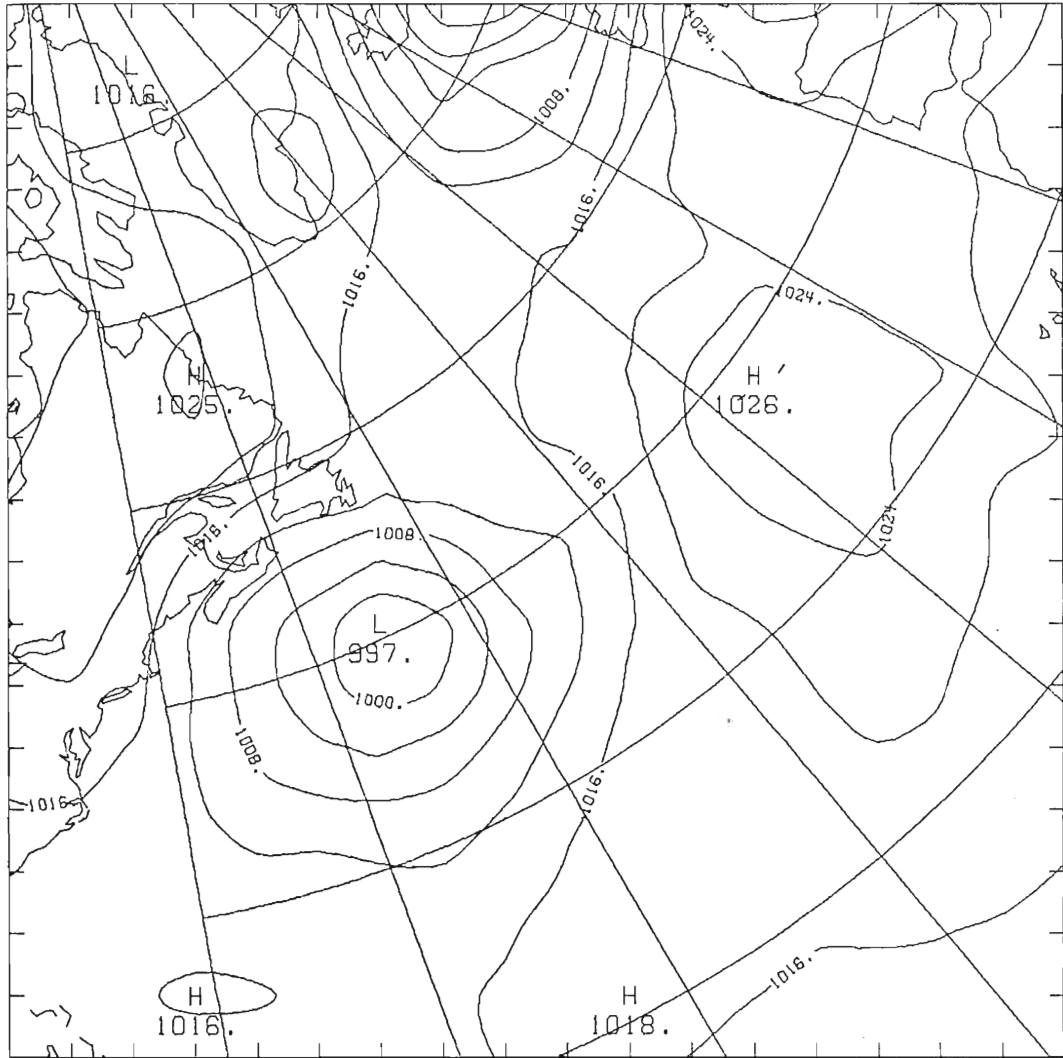


Fig.5b Same as Fig. 5a but for OBS 8.

ADJUSTED P

ØBS 9

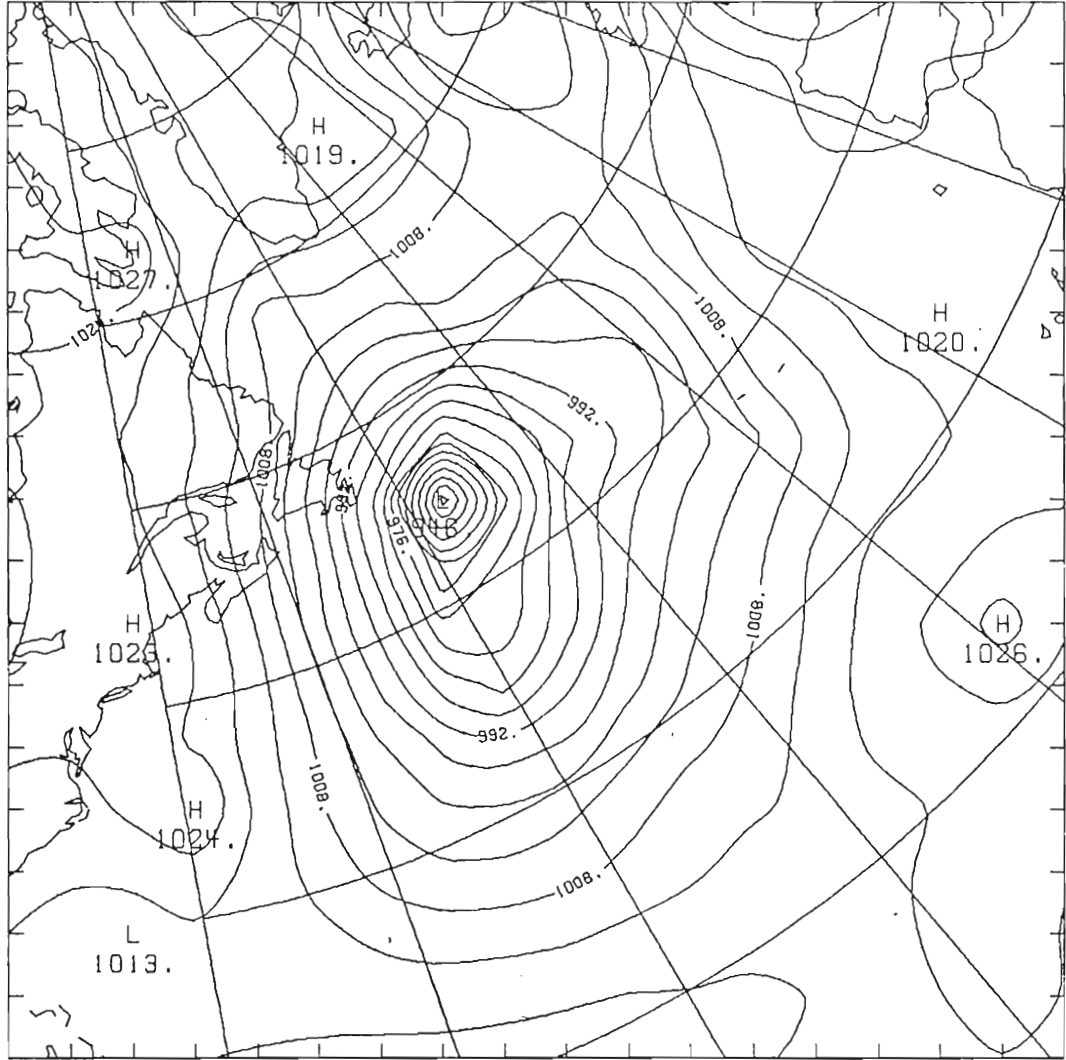


Fig. 5c Same as Fig. 5a but for OBS 9.

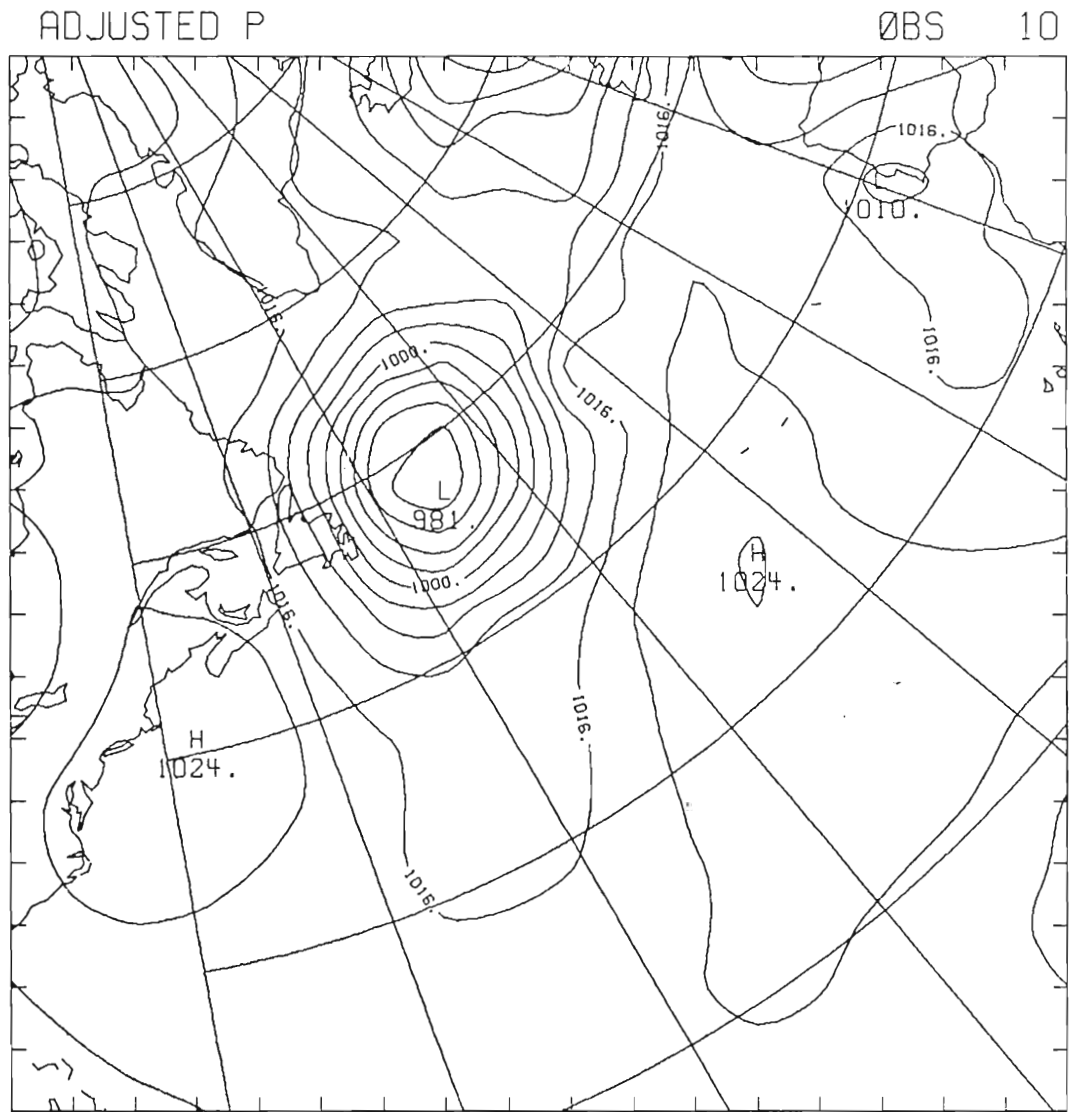


Fig.5d Same as Fig. 5a but for OBS 10.

Fig.5d Same as Fig. 5a but for OBS 10.

ADJUSTED P

OBS 11

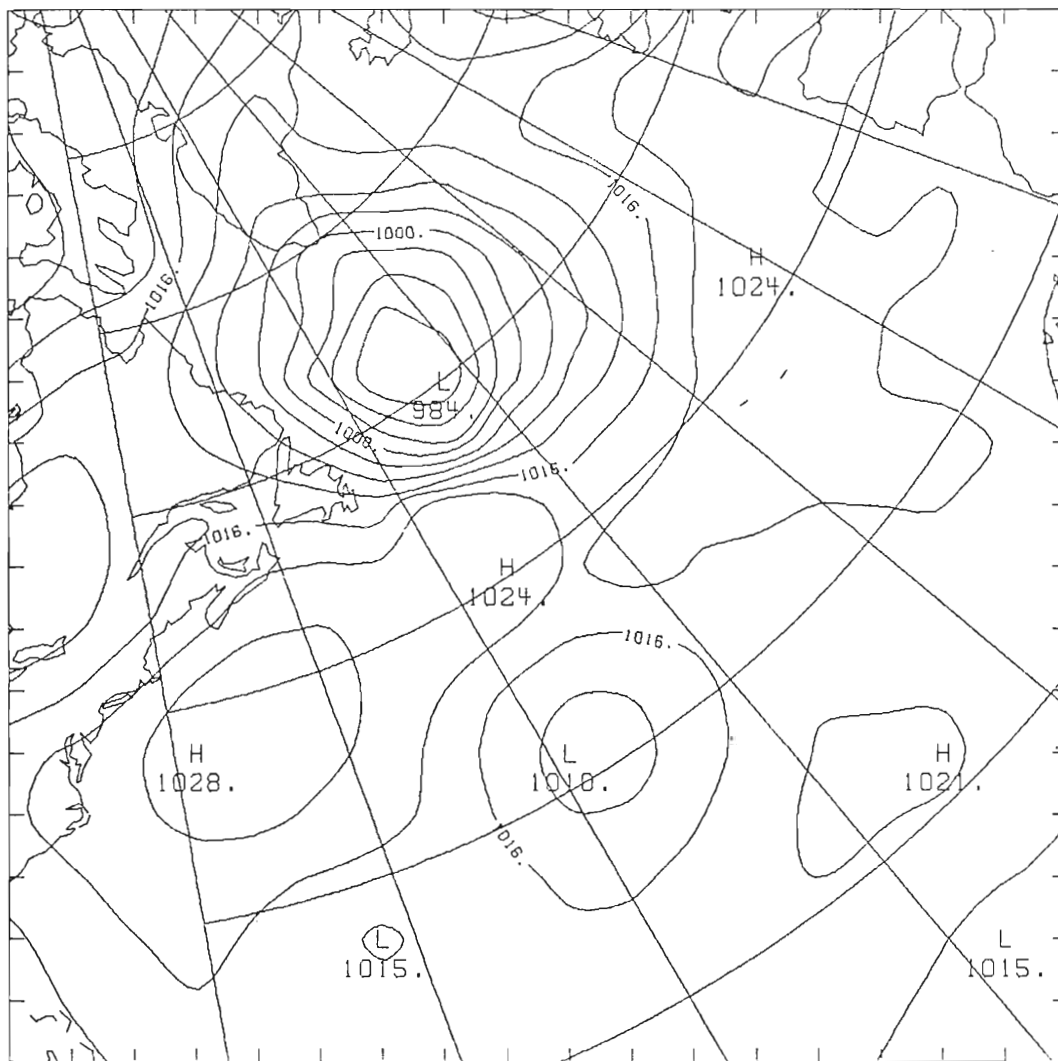


Fig.5e Same as Fig. 5a but for OBS 11.

Fig.5e Same as Fig. 5a but for OBS 11.

geostrophic vorticities, i.e. $F_{ij} = 1.0$ (Figures 6a-e).

It is possible to see the precursor to the QE II storm 24 hours earlier on September 9, 1978 1200 UT (OBS 7) (Figure 2.a). At this point in time, however, there is quite good agreement between the NMC surface analysis, Gyakum's analysis and the insertion of SEASAT data performed in the present study. For example, the resulting central pressures are 1004 mb (Figure 2.a), Gyakum's 1004 mb and 1000 mb (Figure 5.a). Gyakum obtained a relative of $1.7 \times 10^{-4} \text{s}^{-1}$ while ours was $1.5 \times 10^{-4} \text{s}^{-1}$. The sequence of adjusted pressure fields are shown in Figure 5.a-e.

The ocean liner Queen Elizabeth II was damaged on September 11, 1978 (OBS 10 and OBS 11). It is believed that a more accurate NMC surface analysis for the 24 hours before the time of the damage (September 10, 1978, OBS 8 and OBS 9) may have prevented it. As can be seen from Figure 2.b, the NMC analysis estimates the low pressure south of Newfoundland to be 1003 mb. Using subjectively de-aliased SASS winds and other sources of input data, Gyakum (1983) obtains a "conservative" estimate of the storm center at this time to be 990 mb. One might expect a pressure center deeper than 997 mb obtained after the data insertion done in this study for OBS 8 due to the fact that the surface winds for SASS are much higher than those produced by the reduction-rotation method in the storm area (Figure 5.b). The reason for this discrepancy is that the satellite coverage of the storm area was nearly 3 hours away from the NMC (Figure 5.b). The reason for this discrepancy is that the satellite coverage of the storm area was nearly 3 hours away from the NMC analysis time leading to a weighting of about 0.47 for the relative

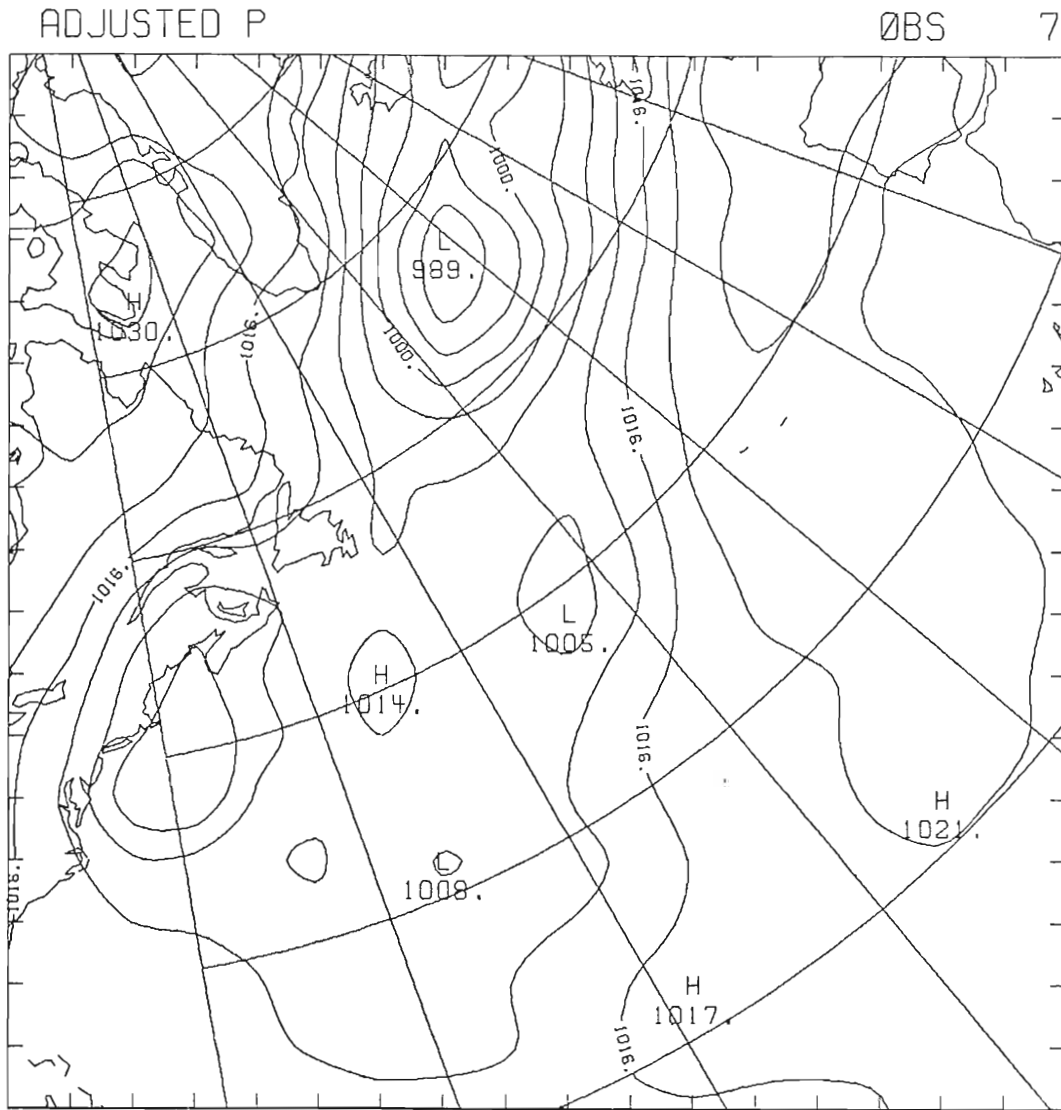


Fig.6a Adjusted surface pressure after substitution ($F_{ij} = 1.0$)

Fig.6a Adjusted surface pressure after substitution ($F_{ij} = 1.0$)
of SASS relative vorticities, OBS 7.

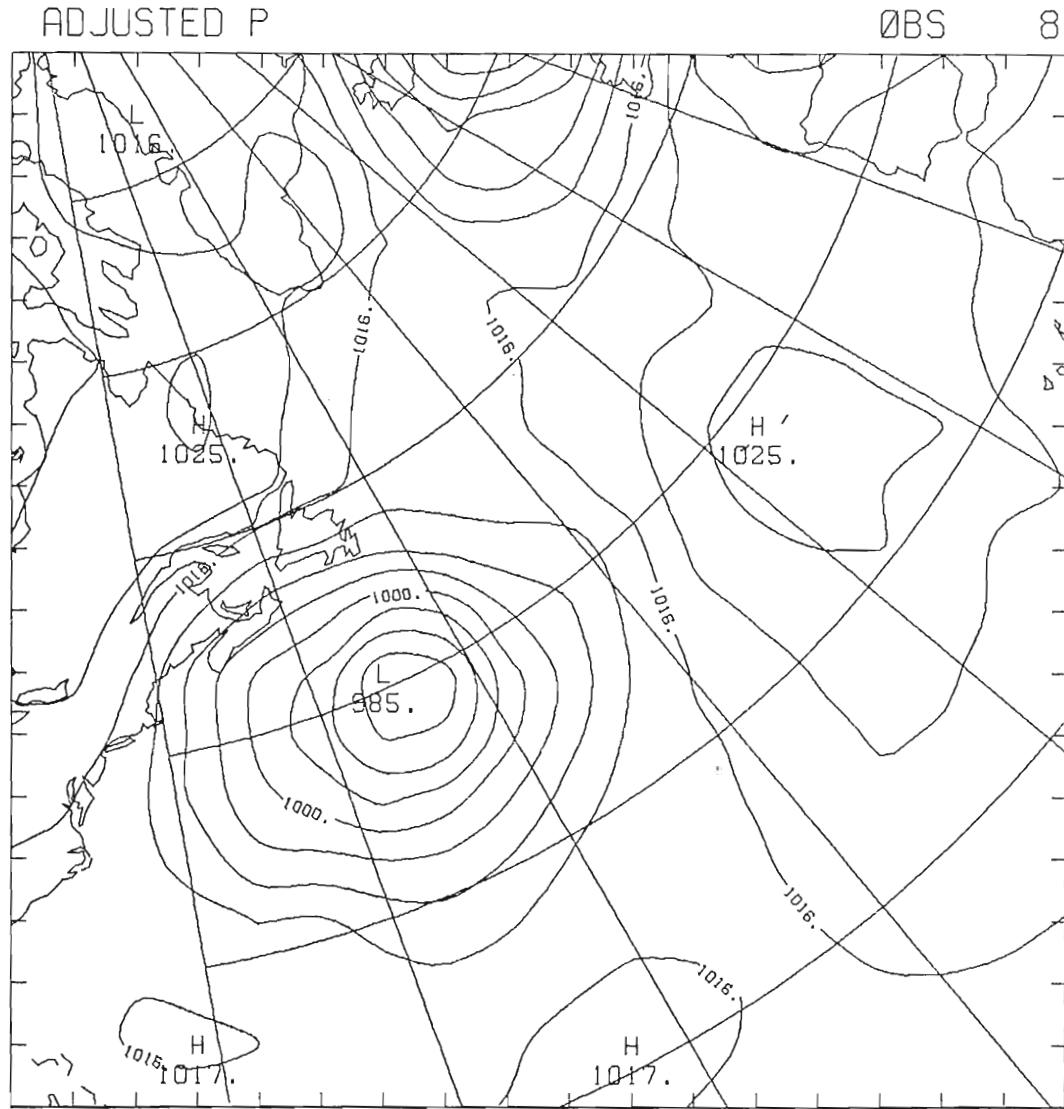


Fig.6b Same as Fig. 6a but for OBS 8.

ADJUSTED P

OBS 9

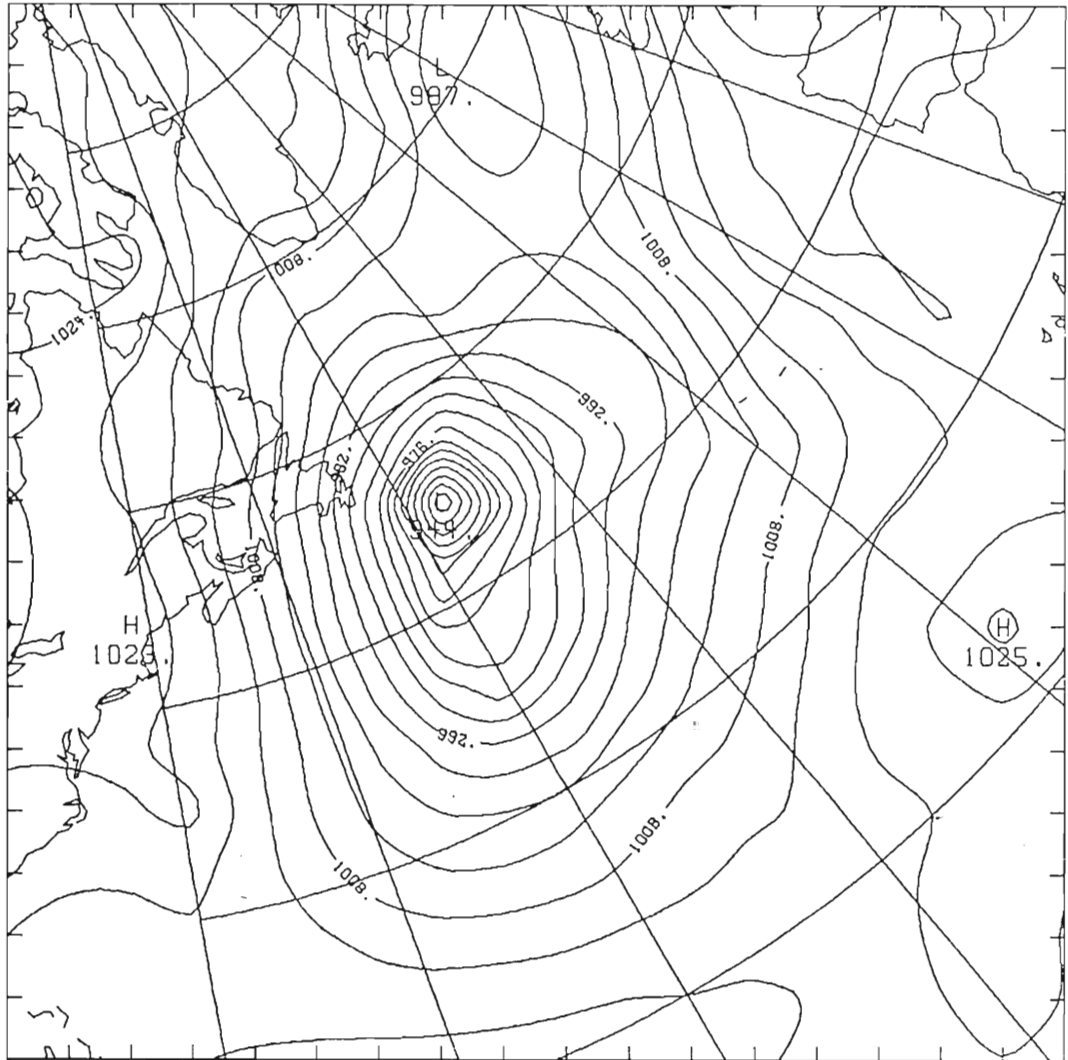


Fig. 6c Same as Fig. 6a but for OBS 9.

Fig. 6c Same as Fig. 6a but for OBS 9.

ADJUSTED P

ØBS 10

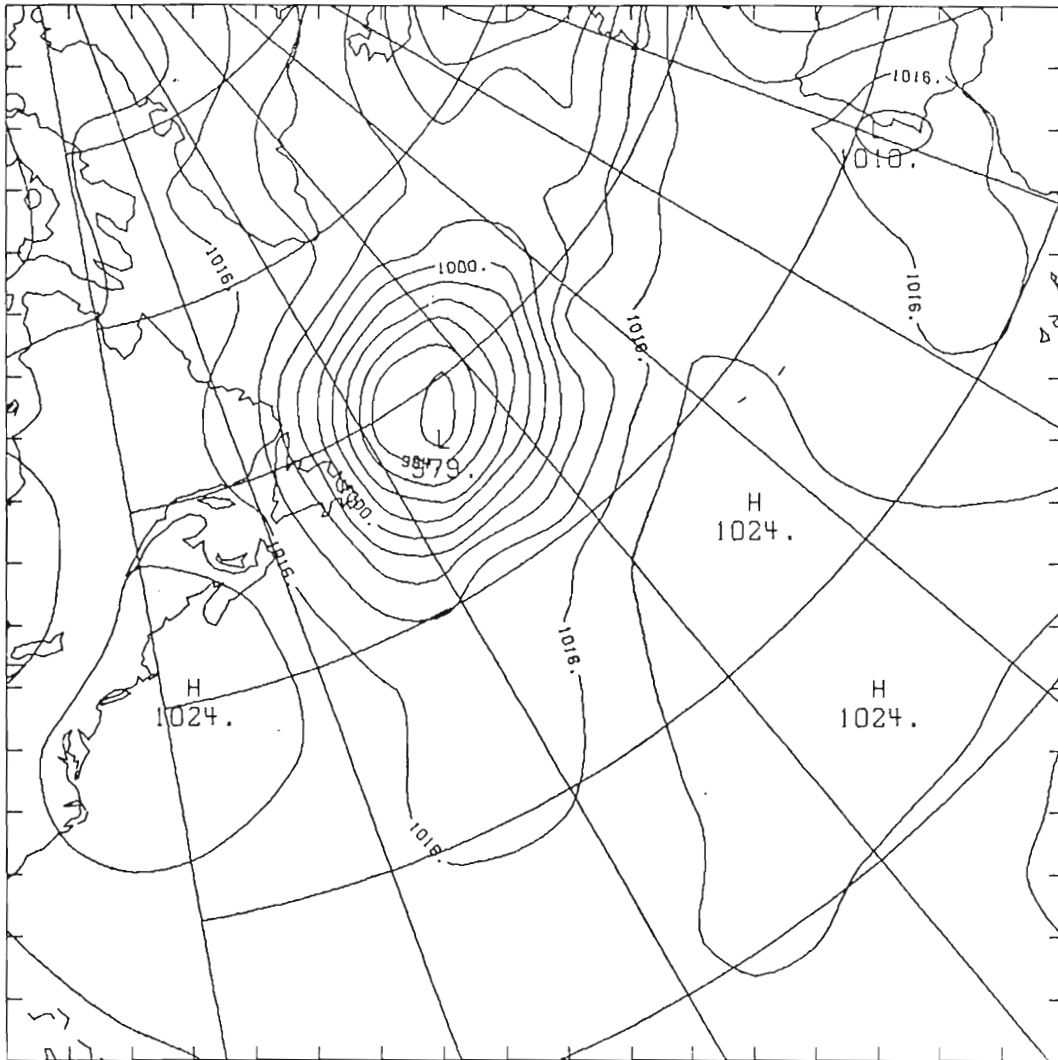


Fig.6d Same as Fig.6a but for OBS 10.

Fig.6d Same as Fig.6a but for OBS 10.

ADJUSTED P

ØBS 11

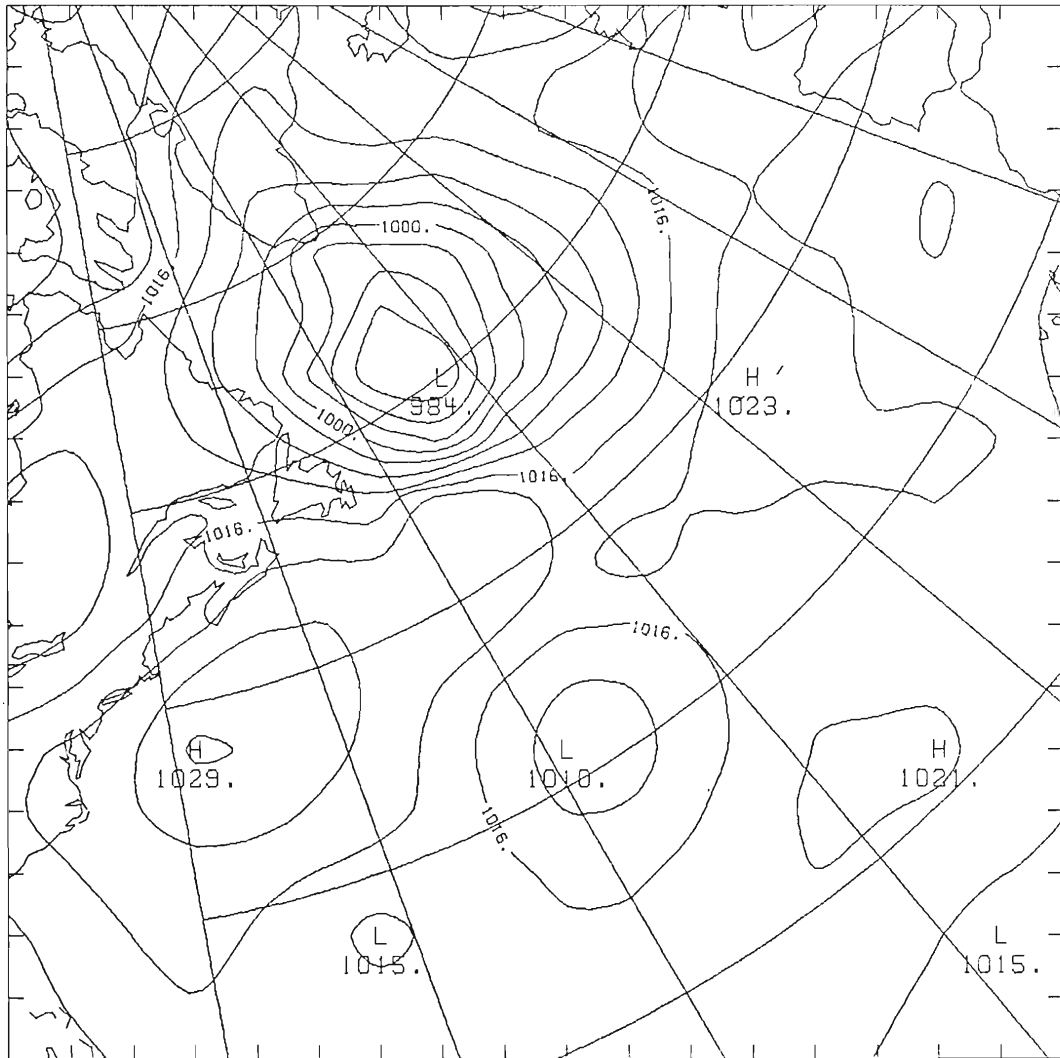


Fig.6e Same as Fig. 6a but for OBS 11.

vorticities calculated from the SASS winds in that region. By changing the weighting function to be 1.0 (thus substituting the SASS vorticity for the NMC vorticity), a central pressure of 985 mb is obtained (Figure 6b).

As was implied above, the NMC analysis for September 10, 1978 1200 UT (OBS 9) was the most critical in that it could have predicted the severe storm that the QE II would encounter approximately 24 hours later. It should be noted, again, that the final NMC surface analysis calculated a pressure of 980 mb, not 998 mb, for the storm center for OBS 9. The 998 mb value (Figure 2c) is the result of smoothing done in converting from the finer mesh grid used in the NMC final analysis to the more coarse NMC octagonal grid from which our surface pressure data were obtained.

The central low pressure of 946 mb obtained after insertion of the SASS winds (Figure 5c) is a significant improvement over the 980 mb value from NMC and also agrees with the value obtained by Gyakum (1983). Gyakum estimated the relative vorticity from the SASS winds by using a finite difference method on a $1^{\circ} \times 1^{\circ}$ grid. He obtained a value for the storm center of $5 \times 10^{-4} \text{s}^{-1}$. Although our method produced a value of about $7.5 \times 10^{-4} \text{s}^{-1}$, the resulting central pressure is still the same as Gyakum's estimate. This is probably due to the influence of neighboring grid points which smoothed out the pressure field due to their distance from the storm center and their correspondingly higher pressures. the pressure field due to their distance from the storm center and their correspondingly higher pressures.

By September 11, 1978 0000 UT (OBS 10), the low pressure center of the storm had increased to approximately 980 mb. The storm at this time was still extremely violent, with winds above 60 knots and wave heights of 50 feet or more (Ernst, 1981). By this time, the NMC analysis had accurately described the severity of the storm; attributing a value of 983 mb to the storm center (Figure 2.d). The SASS data insertion technique provided a similar value of 981 mb (Figure 5.d). One might also notice that a rather large high pressure system covering the upper right section of Figure 2.d has been replaced by a fairly flat region of pressures between 1017 mb and 1021 mb (Figure 5.d). This is significantly lower than the value of 1030 mb in NMC analysis. However, the portion of the high pressure system extending over the lower right half of Figure 7.d agrees well with the original NMC analysis. If one considers the SASS wind vectors (Figure 7), it is apparent that the center of the anti-cyclonic circulation is the same as that indicated by the NMC analysis. The reason for the discrepancy in magnitude of this high pressure region is not clear.

The last NMC analysis that was subjected to the SASS data insertion was 12 hours later, September 11, 1200 UT (OBS 11) (Figure 2.e). The NMC analysis is considered to be accurate and the adjusted analysis (Figure 5.e) agrees well, differing only by a somewhat shallower northern edge of the low pressure. Since the NMC analyses for OBS 10 and OBS 11 are very similar and are considered somewhat shallower northern edge of the low pressure. Since the NMC analyses for OBS 10 and OBS 11 are very similar and are considered

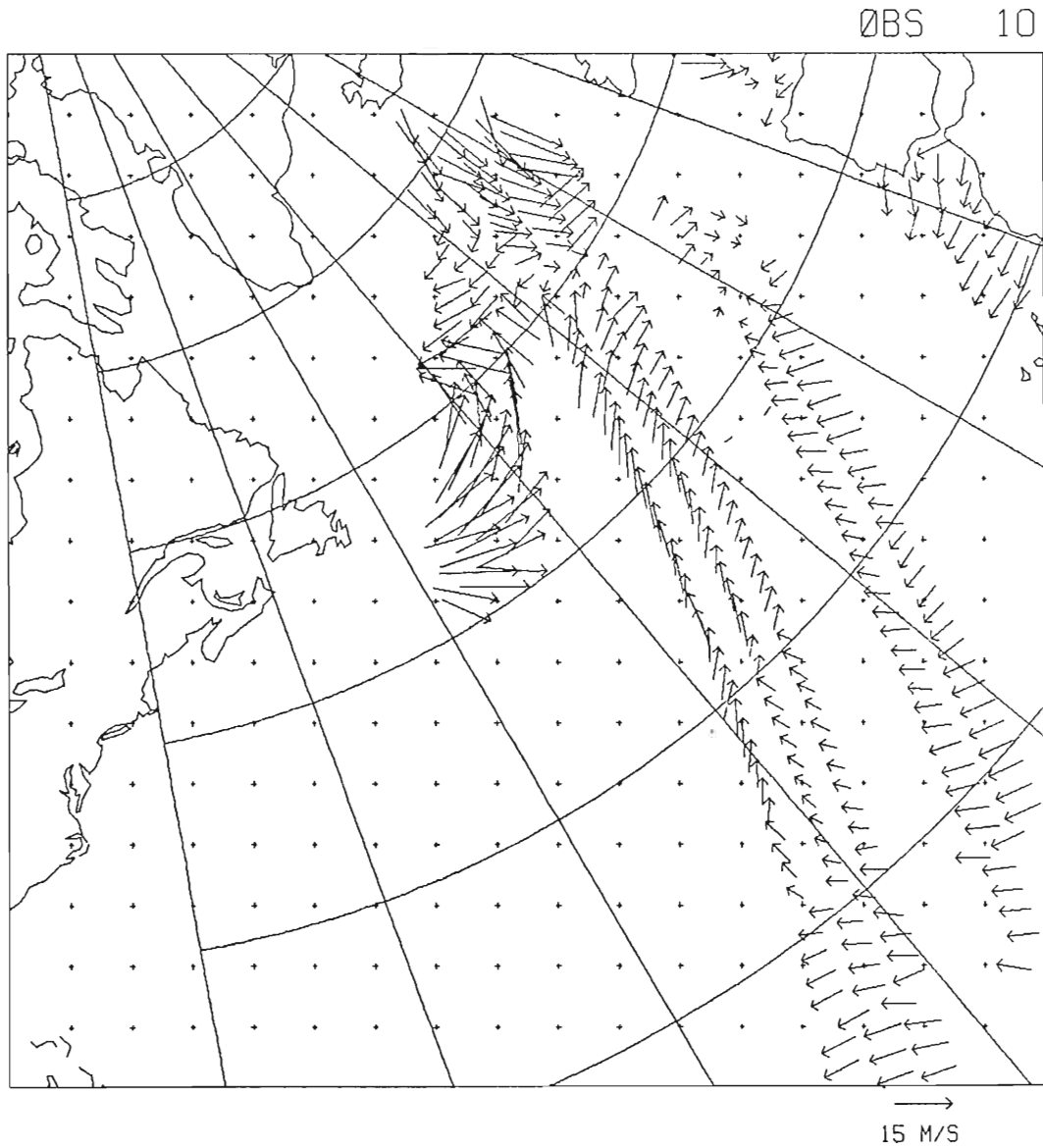


Fig. 7 SASS wind vectors for OBS 10. Note that only

Fig. 7 SASS wind vectors for OBS 10. Note that only every other arrow is plotted for clarity.

to be correct and the adjusted analyses are quite different from each other; some explanation is necessary. That is, why does the adjusted pressure field for OBS 11 fail to provide a northern edge that is as steep as the NMC analysis, even though the SASS winds are slightly higher than the reduced-rotated geostrophic winds (Figure 3e). Figure 10, the wind vectors for OBS 11, provides the answer. The SASS vorticity calculations near the storm center include points from two different orbits. It appears that there are several places north of the storm where the direction of adjacent winds differ by about 90°. This would clearly present problems for the SASS vorticity calculations.

The most critical tests for this assimilation technique are OBS 8 and OBS 9, i.e. the 2 analyses corresponding to the 24 hours before the damage occurred to the Queen Elizabeth II.

The weights for the SASS vorticities for the storm region of OBS 8 were less than 0.50. This led to a somewhat high value of 997 mb for the storm since the NMC value was given a weight of slightly more than 0.50. The fully weighted ($F_{ij} = 1.0$) pressure field produced a value of 985 mb; less than Gyakum's estimate by 5 mb. There is, however, no surface truth to verify how "conservative" Gyakum's estimate was.

Had the weight for SASS vorticity near the storm center of OBS 9 been 1.0 (i.e. had the satellite passed over much later or earlier), the resulting pressure field may have been much higher. Had the weight for SASS vorticity near the storm center of OBS 9 been 1.0 (i.e. had the satellite passed over much later or earlier), the resulting pressure field may have been much higher than the 946 mb value obtained. This would cause a much less

significant improvement in the adjusted pressure field.

These two examples, combined with the fact that no marked errors are introduced by the full substitution method for any of the 5 analysis times, lead one to conclude that the full substitution method is best, i.e., we should use the SEASAT winds whenever possible.

The most critical parameter in the entire insertion method is the selection of the size of the square in which the SASS relative vorticity estimate is calculated. Since the winds which will be used in this vorticity calculation are chosen so as to be nearest the corners of the square, this is not a surprising result.

For most synoptic scale features, small variations in the size of this square cause at most about 10 mb differences (Figure 8).

For regions of intense gradients (e.g. the QE II storm on OBS 9), variations in the size of the square, even small ones, can lead to large changes in the resultant pressure field in the region of the gradient. In these circumstances, the choice of the size of the square becomes subjective with the final choice being that which results in the most accurate agreement with the wind vector field and any other known data. Figure 9 illustrates the effect of selecting a slightly larger size for the square in which the SASS vorticity is calculated for OBS 9. The vorticity calculation at the storm center produced a value of $4.2 \times 10^{-4} \text{s}^{-1}$, but smoothing from neighboring grid points has caused the low center pressure to fill storm center produced a value of $4.2 \times 10^{-4} \text{s}^{-1}$, but smoothing from neighboring grid points has caused the low center pressure to fill

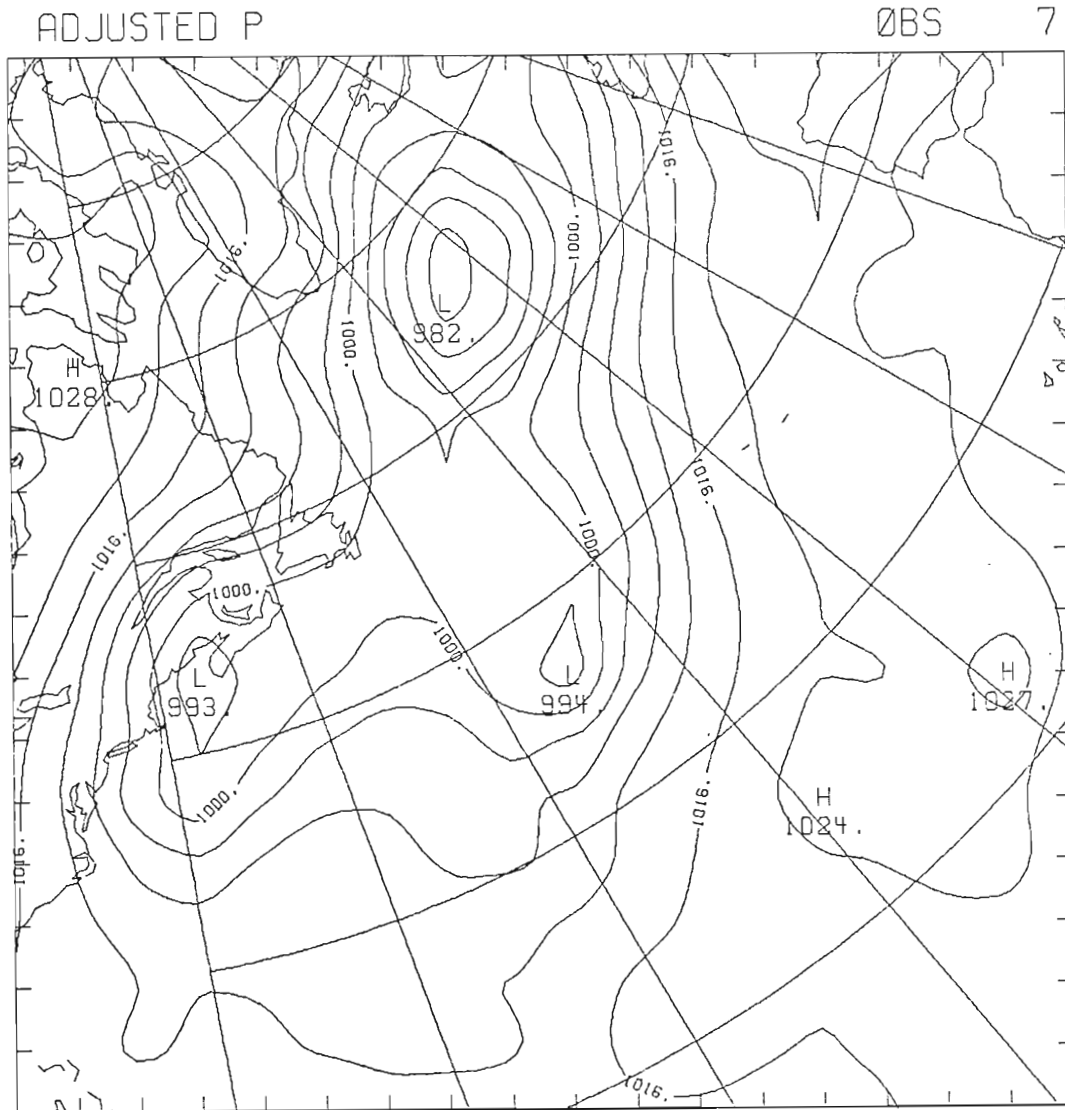


Fig. 8 Same as Fig. 6a but for slightly larger square

Fig. 8 Same as Fig. 6a but for slightly larger square
in which SASS relative vorticity is calculated.

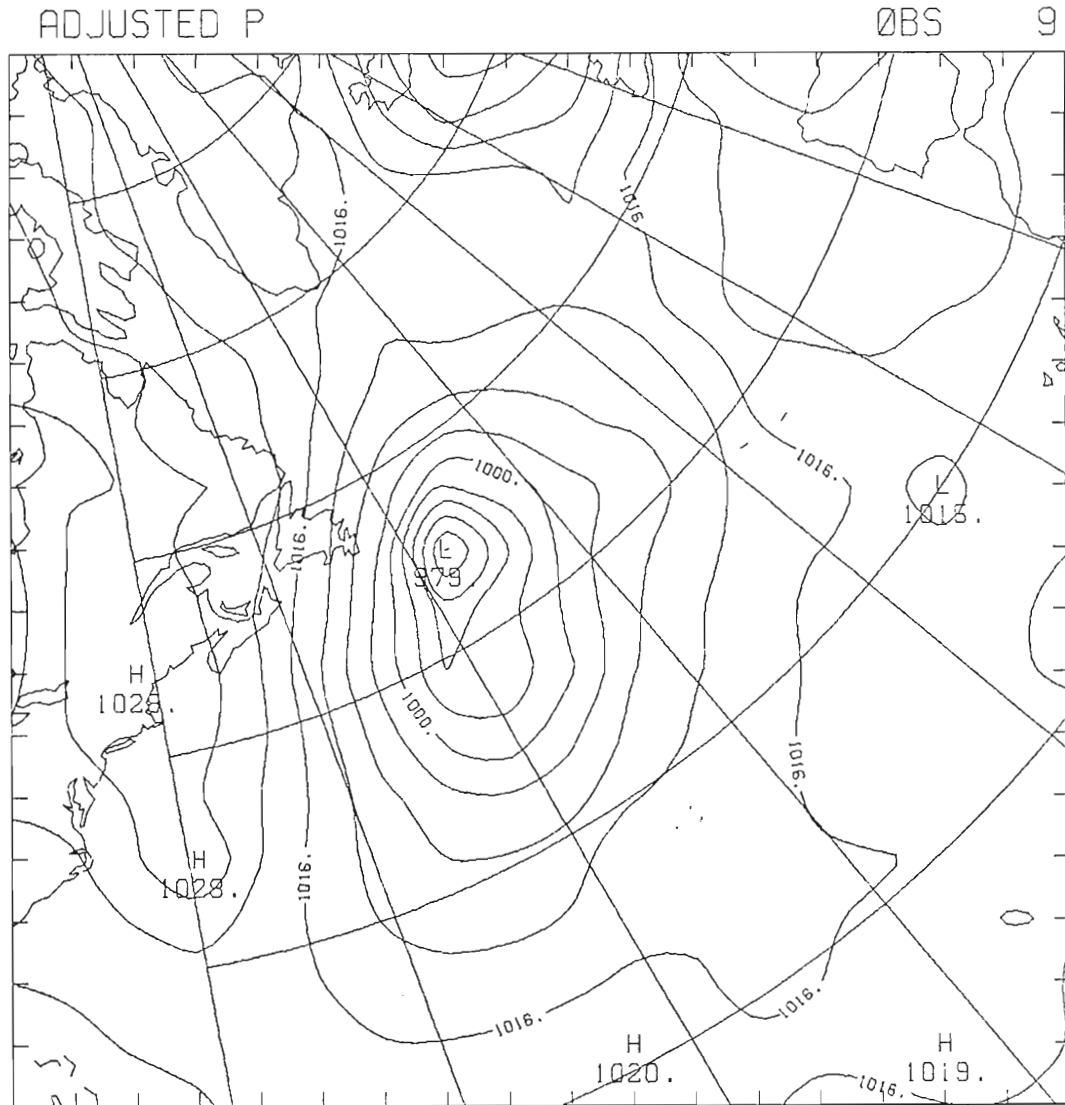


Fig. 9 Same as Fig. 6c but for slightly larger square in which SASS relative vorticity is calculated.

Fig. 9 Same as Fig. 6c but for slightly larger square in which SASS relative vorticity is calculated.

in to a 979 mb value. This pressure should be lower based on other results. For example, at the storm center in OBS 10, the low of 983 mb had a corresponding vorticity of $2.0 \times 10^{-4} \text{ s}^{-1}$. Recall that Gyakum's calculation of the vorticity at the storm's peak was 5.0×10^{-4} and had a 945 mb pressure associated with it. Clearly then, a vorticity of $4.2 \times 10^{-4} \text{ s}^{-1}$ should produce a low pressure lower than 979 if the surrounding grid points accurately reflect the pressure gradient since the scale is the same. Assuming a simple linear relationship between the storm center pressure and the vorticity, a value of $4.2 \times 10^{-4} \text{ s}^{-1}$ should lead to a pressure of about 955 mb.

Conclusions

In order to test the possibility of improving surface pressure analyses using SEASAT-A scatterometer winds, it was first determined that the SASS winds were more accurate than winds derived from NMC surface pressure fields in the region of the QE II storm. This was because the NMC pressure field did not exhibit a steep enough gradient in the storm region.

Sea level pressure fields and SEASAT-A scatterometer surface wind measurements were assimilated using a variational formulation. Relative vorticity estimates were calculated using each of these two data sets.

The technique used for calculating the relative vorticity estimates using SASS surface winds resulted in improvement of NMC surface pressure fields where they were grossly in error, namely September 10 1200 UT at the QE II storm. However, the technique was dependent on the size of square chosen in which to perform this calculation. The correct fields were chosen subjectively after calculations using different size squares were made. The calculations involved the objective selection of SASS wind vectors nearest to the four corners of the squares, however, a higher resolution pressure grid may allow more accurate and less noisy assimilation of SASS winds.

A difference functional composed of a model which is constrained such that 1) the difference between the relative vorticity from the data and the relative vorticity resulting from the variational formulation is minimized and 2) the kinetic energy of the resultant pressure field is minimized, is constructed. The kinetic energy constraint also acts as a smoothing operator.

Each of the relative vorticity estimates calculated from SASS surface winds were given a weight depending on the nearness in time to the NMC analysis time for which the original pressure analysis was made. This weighting was done in order to test the current NMC practice of considering all data within a ± 3.0 hour time window from the analysis time as being synoptic.

The "equivalent time averaging" concept was applied to the SASS observations within the 6 hour time window used by the NMC. This effectively causes more of the observations to "become synoptic" at the NMC analysis time. Consequently, more SASS vorticity calculations acquire a weight of 1.0. For each of the 5 analysis times investigated in this study, the method of equivalent time averaging produces virtually the same result as treating each SASS observation as asynoptic and subsequently giving a weight which depends on the amount of time it differs from the analysis time. It is important to note, however, that the SASS data coinciding with the QE II storm at its peak (OBS 9), was only a short time from the NMC analysis time. Therefore, it was given a coinciding with the QE II storm at its peak (OBS 9), was only a short time from the NMC analysis time. Therefore, it was given a

weight of nearly 1.0 with either method. If the satellite had passed over just one hour sooner, the weight could have been much less with the "asynoptic method" resulting in a much more shallow low pressure and a poorer analysis. The equivalent time averaging method very possibly would still have resulted in a weight of 1.0.

There are not many major differences between setting all the weights equal to 1.0 or retaining them as is. This fact, coupled with the possibility of losing a more accurate analysis of a storm by retaining the weights, forces one to conclude that giving full weight, i.e. substituting the SASS relative vorticity estimates wherever they occur, is the most correct method. This agrees with the NMC practice of considering all data within a ± 3.0 hour time window as being synoptic. In reality, so many sources of data are available for the analyst that a choice would not actually have to be made between the two data sets. What this study does, perhaps, is support the idea that a great deal of weight could be given satellite scatterometer wind measurements if they were available in real time.

The simple model presented here has been shown to be an effective way of assimilating satellite wind data with surface pressure fields at the ocean surface. The model only requires 2 sources of input data and can result in similar pressure fields to those obtained by more complex methods.

those obtained by more complex methods.

REFERENCES

- Anthes, R. A., Y. H. Kuo, and J. R. Gyakum, Numerical simulations of a case of explosive marine cyclogenesis, Mon. Wea. Rev., 111, 1174-1188, 1983.
- Boggs, D. H., Seasat Scatterometer Geophysical Data Record (GDR) Users' Handbook, 622-232, Jet Propulsion Laboratory, Pasadena, Calif., 1982.
- Brown, R. A., Similarity parameters from first-order closure and data, Boundary-Layer Meteorol., 14, 381-396, 1978.
- Cane, M., and V. J. Cardone, The potential impact of scatterometry on oceanography: A wave forecasting case, in Oceanography from Space, edited by J. F. R. Gower, pp. 587-595, Plenum Press, New York, 1981.
- Clarke, R. H., and G. D. Hess, On the relation between surface wind and pressure gradient, especially in lower latitudes, J. Phys. Oceanogr., 9, 325-339, 1975.
- Duffy, D. G. and R. Atlas, The impact of SEASAT-A scatterometer data on the numerical prediction of the QE II storm, Submitted to J. Geophys. Res.
- Gyakum, J. R., On the evolution of the QE II storm. I: Synoptic aspects, Mon. Wea. Rev., 111, 1137-1155, 1983.
- Hasse, L., and V. Wagner, On the relationship between geostrophic and surface wind at sea, Mon. Wea. Rev., 255-260, 1971.
- Hoffman, R. N., SASS wind ambiguity removal by direct minimization, Mon. Wea. Rev., 110, 434-445, 1982.
- Jenne, R. L., The NMC octagonal grid, National Center for Atmospheric Research, Boulder, Colo., 1970.
- Jones, W. L., L. C. Schroeder, D. H. Boggs, E. M. Bracalante, R. A. Brown, G. J. Dome, W. L. Pierson, and F. J. Wentz, The SEASAT-A satellite scatterometer: The geophysical evaluation of remotely sensed wind vectors over the ocean, J. Geophys. Res., 87, 3297-3317, 1982.
- Brown, G. J. Dome, W. L. Pierson, and F. J. Wentz, The SEASAT-A satellite scatterometer: The geophysical evaluation of remotely sensed wind vectors over the ocean, J. Geophys. Res., 87, 3297-3317, 1982.

- Lame, D. B., and G. H. Born, SEASAT measurement system evaluation: Achievements and limitations, J. Geophys. Res., 87, 3175-3178, 1982.
- Muller, P., and C. Frankignoul, Direct atmospheric forcing of geostrophic eddies, J. Phys. Oceanogra., 11, 287-308, 1981.
- Overland, J. E., R. A. Brown, and C. D. Mobley, METLIB-A Program library for calculating and plotting marine boundary layer wind fields, NOAA Technical Memorandum ERL PMEL-20, 82 pp., Pacific Marine Environmental Laboratory, Seattle, 1980.
- Pedlosky, J., Geophysical Fluid Dynamics, 624 pp., Springer-Verlag, New York, 1982.
- Pierson, W. J., Winds over the ocean as measured by the scatterometer on SEASAT, in Oceanography from Space, edited by J.F.R. Gower, pp. 563-571, Plenum Press, New York, 1981.
- Pierson, W. J., The measurement of the synoptic scale wind over the ocean, J. Geophys. Res., 88, 1683-1708, 1983.
- Sanders, F. and J. R. Gyakum, Synoptic-dynamic climatology of the "bomb", Mon. Wea. Rev., 108, 1589-1606, 1980.
- Sasaki, Y., Some basic formalisms in numerical variational analysis, Mon. Wea. Rev., 98, 875-883, 1970.
- Thomas, A. M., Air-sea interaction study using STREX data, 108 pp., Univ. of Washington, Seattle, 1983.
- Woiceshyn, P. M., M. G. Wurtele, D. H. Boggs, L. F. McGoldrick, S. Peteherych, A new parameterization of an empirical model for wind/ocean scatterometry, Submitted to J. Geophys. Res.
- Wurtele, M. G., P. M. Woiceshyn, S. Peteherych, M. Barowski, and W. S. Appleby, Wind direction alias removal studies of SEASAT scatterometer derived winds, J. Geophys. Res., 87, 3365-3377, 1982.
- Yu, T. W. and R. D. McPherson, Global data assimilation experiments with scatterometer winds from SEASAT-A, Mon. Wea. Rev., 112, 368-376, 1984.